

**CHARACTERIZATION AND DYNAMIC MODELING OF AEROSOLS  
USING ATMOSPHERIC REMOTE SENSING TECHNIQUES IN NIGER DELTA,  
NIGERIA.**

**By**

**CHUKWUDOBE, LEO ODIMBU (B.Sc. UNIJOS, M.Sc. MOSCOW)**

**20134871238**

**A THESIS SUBMITTED TO THE POSTGRADUATE SCHOOL**


**FEDERAL UNIVERSITY OF TECHNOLOGY, OWERRI.**

**IN PARTIAL FULFILLMENT OF THE REQUIREMENTS FOR THE  
AWARD OF DEGREE (MASTER OF SCIENCE), M.Sc. IN GEOPHYSICS**

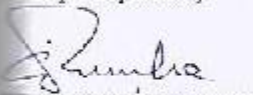
**JUNE, 2021**

## CERTIFICATION

This is to certify that this work "Characterization and Dynamic Modeling of Aerosols using Atmospheric Remote Sensing Techniques in Niger Delta, Nigeria" was carried out by **Chukwudobe, Odumbu Leo (20134871238)** in partial fulfillment for the award of the degree M.Sc in Geophysics in the Department of Geology of the Federal University of Technology Owerri.

  
Dr. A.I. Opara  
(Principal Supervisor)

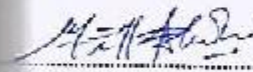
13/06/2021  
Date

  
Dr. C.N. Okereke  
(Co-Supervisor)

10/06/2021  
Date

  
Dr. A.I. Opara  
(Head of Department)

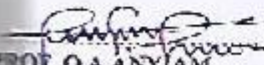
13/06/2021  
Date

  
Prof. C.C.Z. Aknollisa  
(Dean of SOPS)

28/7/2021  
Date

Prof. C.C. Eze  
(Dean, Postgraduate School)

.....  
Date

  
Prof. O.A. ANYIAM  
(External Examiner)

15-6-2021  
Date

## **DEDICATION**

**To**

The Lord Almighty, for leading and guiding me throughout the entire program.

## **ACKNOWLEDGEMENTS**

I wish to thank God for seeing me through, throughout my academic journey since 1985.Chukwudalu.

Furthermore, I wish to use this medium to express my heartfelt gratitude to all those who in one way or the other assisted me in the course of this project. Worthy of mention are the amiable lecturers and staff of the great department of Geology, and the School of Physical Sciences (SOPS), FUTO. I acknowledge the efforts of my supervisors, Dr. A.I. Opara and Dr. C.N. Okereke who painstakingly read and corrected this piece of research work to ensure that it came out in this form. I acknowledge the indelible efforts of the Head of Department of Geology, in the person of Dr. A.I. Opara, the Dean School of Physical Sciences, in the person of Prof. C.Z Akaolisa, and the Departmental PG Coordinator in the person, of Dr. C.N Okereke. My appreciation also goes to Prof. K.K Ibe, Prof. O.C Okeke, Prof.S.O Onyekuru, Dr.I.Njoku, Mr. Essien A.G, Dr. S.I Ibeneme, and all other members of staff for their support.

I also want to thank Dr. N.D Onyeuwaoma who assisted in the acquisition of data used for this research work, his encouragement and enhancement of my skills in satellite aerosol and atmospheric studies are not forgotten.

Also, I want to express unalloyed appreciation to my parents Mr. & Mrs. A.C. Mokuwonye, who first taught me that hard work begets success and integrity. Thank you very much. My siblings are not left out, Kevin, Augusta, Cynthia, & Vera thank you all for your supports at various times.

To my colleagues at FUTO Owerri, especially Mr. Steven Adikwu, Aquila Chukwuemeka, and others who believed in me, your encouragements mustered me to greater success.

## TABLE OF CONTENTS

Certification	i
Dedication	ii
Acknowledgements	iii
Table of Contents	v
List of Tables	ix
List of figures	x
Abstract	xii

### CHAPTER ONE: INTRODUCTION

1.1 General Overview	1
1.1.1 Formation of Aerosols	3
1.1.2 Classification of Aerosol	4
1.1.3 Removal of Aerosol Particles from the Atmosphere	5
1.1.4 Effects of Aerosols on the Earth Systems	7
1.2 Aim and Objectives	9
1.3 Statement of the problem.	9
1.4 Justification of study	9
1.5 Scope of study	10

### CHAPTER TWO: LITERATURE REVIEW

2.1 Review of related works	11
-----------------------------	----

2.2	Remote Sensing	20
2.2.1	Atmospheric Satellite Remote Sensing	22
2.2.2	Scattering of Radiation	24
2.2.3	Characterization of Aerosols	25
2.2.4	Scattering and Absorption of light by Aerosol	25
2.2.5	Advantages of In-situ measurements	25
2.2.6	Disadvantages In-situ measurements	26
2.2.7	Advantages of remote sensing from Satellites	26
2.2.8	Disadvantages remote sensing from Satellites	26
2.3.1	Oil Spill/Gas Flaring	26
2.3.2	Extent of the problem	27
2.3.3	Causes	28
2.3.4	Consequences	29
2.3.5	Gas Flaring in Nigeria	29
2.3.6	Environmental Implication	30
2.3.6a	Climate Change	30
2.3.6b	Acid Rain	31
2.3.6c	Agriculture	31
2.3.7	Health Implications	32
2.3.7a	Adverse Effects	32
2.3.7b	Hematological Effects	32
2.3.7c	Economic Loss	32
2.3.7d	Pollution	33

2.3.8	Impacts of waste flaring associated gas from oil drilling sites	33
2.4	Climate Change	33
2.3.9	Global Carbon Cycle Overview	34
2.3.10	Methane Cycle	36
2.3.10	Nitrous Cycle	37

### **CHAPTER THREE: MATERIALS AND METHODS**

3.1	Sampling areas	40
3.1.1	Data Sets	40
3.2	Data Acquisition	41
3.3	Ozone Monitoring Instrument (OMI)	41
3.4	Atmospheric Infrared Sounder	42
3.5	NOAA Hybrid Single-Particle Integrated Trajectory (HYSPLIT)	43
3.6	Location and Physiography of the Study area	44
3.7	Geology of the Study Area	44
3.7.1	Vegetation	46
3.7.2	Relief	46
3.7.3	Climate	47
3.8	Model for Data Integration	49
3.9	Workflow	50

### **CHAPTER FOUR: RESULTS AND DISCUSSION**

4.1	Presentation	51
-----	--------------	----

4.2	Discussion	72
-----	------------	----

## **CHAPTER FIVE: CONCLUSION AND RECOMMENDATION**

5.1	Conclusion	81
-----	------------	----

5.2	Recommendation	84
-----	----------------	----

5.3	Contribution to Knowledge	85
-----	---------------------------	----

<b>REFERENCES</b>		<b>86</b>
-------------------	--	-----------

## LIST OF TABLES

Table 1.1: Aerosol classification	5
Table 1.2: Aerosol particle sizes and their fall speed	7
Table 3.1: Data Instruments and uses	40
Table 4.1: Distance of deposition of particles	61
Table 4.2: Percentage (%) annual variation between 2013 and 2015	66
Table 4.3: Statistical inference from the means of the years under study	67
Table 4.4: Variation between loadings during different seasons	68
Table 4.5: Variation of loadings between Dry and Rain Seasons	69
Table 4.6: Percentage Difference of Atmospheric Species in the Various Locations	71

## LIST OF FIGURES

Fig. 1.1: Production, growth, and removal of atmospheric aerosols	3
Fig. 1.2: Aerosol formation	3
Fig. 1.3: Drag force against gravity acting on an aerosol particle	6
Fig. 1.4: Scattering of solar radiation beam	8
Fig 2.1: Images of Gas Flaring in the Niger Delta	30
Fig. 2.2: Simplified Schematic Overview of Global Carbon Cycle	36
Fig. 2.3: Simplified Schematic Overview of Global Methane Cycle	37
Fig. 2.4: Simplified Schematic Overview of Global Nitrous Cycle	39
Fig. 3.1: Map showing locations of the study area	44
Fig. 3.2: Geological Map of Niger Delta.	45
Fig. 3.3: Data Integration	49
Fig. 3.4: Workflow	50
Fig. 4.1: Time series of the plot of CH <sub>4</sub> emission from January 2013-June 2015	51
Fig.4.2: Time series of the plot of SO <sub>2</sub> emission from January 2013-June 2015	52
Fig.4.3: Time series of the plot of CO emission from January 2013-June 2015	53
Fig. 4.4: Time series of the plot of NO <sub>2</sub> emission from January 2013-June 2015	54
Fig. 4.5: HYSPLIT model showing the concentration of pollutants in Oguta	56
Fig. 4.6: HYSPLIT model showing the concentration of pollutants in PHC	57
Fig. 4.7: HYSPLIT model showing the concentration of pollutants in Warri	58
Fig 4.8: HYSPLIT model showing the concentration of pollutants in Eket	59
Fig 4.9: HYSPLIT model showing the concentration of pollutants in Akpabuyo	60

Fig 4.10: Spatial distribution of methane emission within the Niger Delta over the sample period	62
Fig 4.11: Spatial distribution of carbon monoxide emission within the Niger Delta over the sample period	63
Fig 4.12: Spatial distribution of Nitrogen dioxide emission within the Niger Delta over the sample period	64
Fig 4.13: Spatial distribution of Sulphur dioxide emission within the Niger Delta over the sample period	65

## ABSTRACT

Atmospheric aerosols; CO, CH<sub>4</sub>, SO<sub>2</sub>, and NO<sub>2</sub> over the study area were retrieved using remote sensing from the Ozone Monitoring Instrument (OMI) and the Atmospheric Infrared Sounders (AIRS) over two years. The gas trajectories were performed using the Hybrid Single-Particle Lagrangian Integrated Trajectory (HYSPLIT) model at heights: 0, 50m, and 100m above the ground level. Detailed characterization and dynamic modeling were later processed using Giovanni software and analyzed graphically using time series interpretation and statistically using a Z-test. The study revealed that CH<sub>4</sub> concentration in Oguta, Warri, and Akpabuyo outweighs the value in Port Harcourt by 30.7%, 24.9%, and 29.2%, respectively, while the volume occurrence in Port Harcourt outweighs that of Eket by 3.13%. On a temporal scale, the variations in the emission of the gases are insignificant except for Port Harcourt and Eket where the Z-test calculation was 1.76 and 1.8 at a critical value of 1.96 and a P-value of 0.05. This certainly suggests an increasing value of SO<sub>2</sub> in Port Harcourt and Eket by 10.8% and 11.6%. From the results, it can be concluded that CH<sub>4</sub> and CO are the most abundant gases in the Niger Delta while the emissions of NO<sub>2</sub> and SO<sub>2</sub> in all the study locations are insignificant. It is therefore recommended that appropriate environmental legislation and measures for mitigation and reduction of atmospheric emission should be formulated in the study area for environmental sustainability.

Keywords: Atmospheric aerosols, Ozone Monitoring Instrument, Atmospheric Infrared Sounders, Z-test, Emission.

# CHAPTER ONE

## INTRODUCTION

### 1.1 General Overview

For the past decade, Earth-orbiting satellites sensors have provided near-real-time, kilometer resolution data on the global distribution of atmospheric aerosols. The satellites have tried to explain major pollution, dust, and smoke events in stunning detail because atmospheric aerosols are exceptionally well suited for satellite remote sensing. The sun provides a stable light source and the light scattered by aerosols is easily detectable by high resolution, spectral radiation sensors. Aerosol interaction with visible solar radiation through scattering never ceases to offer intriguing, new counter-intuitive optical phenomena and explanations of how nature works. The satellites, as cameras in the sky, have offered a way to visualize and enjoy these phenomena. These unique Earth observations have shown great potential to aid Earth science, air quality management, and disasters management. The global-scale aerosol monitoring has further potential to improve our understanding of aerosol-induced climate effects as a colorful complement to dry but highly useful theory of radiative transfer (Chandrasekhar, 1960). Its applications include air quality management, the detection and forecasting of major dust and smoke events, and the development of aerosol emission inventories.

The study of atmospheric aerosols is a very important element in the understanding of the earth's solar radiation budget, water cycle balance, and climate change dynamics. There are various types of aerosols in nature with varying impacts on the ecosystem. Therefore, its characterization remains the only way to understand which aerosol type is impacting what. There is the need therefore to study and understand the Spatio-temporal variation of these particulates at every

given time in order to predict its occurrence when armed with the right information. In an environment like the Niger Delta where the study of the Spatio-temporal study of aerosols is still scanty or nonexistent, this work becomes a handy source of information and tends to fill up this gap. Hence, in this work, we characterized the aerosol species in the Niger Delta as fine aerosols taking into consideration the climatic belt of the region, and the various economic activities in the region. Because of this, five (5) locations were singled out for studying; they are Eket (Akwa Ibom), Oguta (Imo), Akpabuyo (Cross River), Port-Harcourt (Rivers), Warri (Delta).

Other considerations for this research are that aerosol particles in the atmosphere can scatter and/or absorb earth-bound solar radiation as well as emitted and reflected radiation from the earth, at varying degrees, depending on their characteristic properties, which may be chemical or physical. The understanding of the magnitude of these effects is constrained because there is limited knowledge of the processes that control the distributions as well as the physical, chemical, and optical properties (IPCC, 2007). This is partly due to the instrumental limitations associated with the current aerosol measurement techniques (McMurry, 2000), which can be attributed to modeling limitations (Haung, 2010) and lack of skills in data handling.

Therefore, aerosol(s) is defined as a suspension in air or liquid, or solid particles in the gaseous medium. They are ubiquitous and include dust particles from deserts, sea salt, carbonaceous aerosols from biomass burning, soot, and fossil fuels. They can occur naturally or humanly induced. The natural aerosols are dust, volcanic ashes, pollens, sea salts while the human-induced aerosols are mostly carbonaceous. The natural aerosols are coarse while anthropogenic aerosols are finer.

### 1.1.1 Formation of Aerosols

Aerosols are formed by two major mechanisms. The gas to particle conversions and mechanical and chemical disintegration of solid and liquid earth surfaces as shown in Figure 1.1. The figure shows the process of aerosol production, growth, and removal from the atmosphere. Aerosols

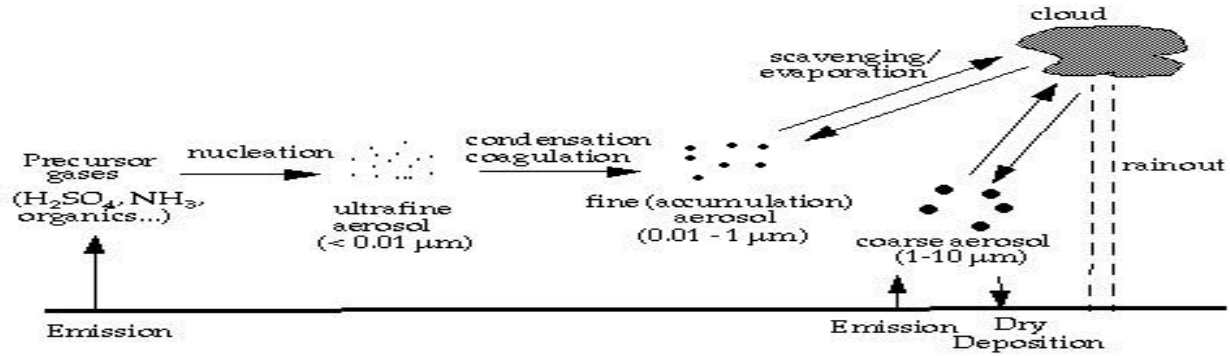
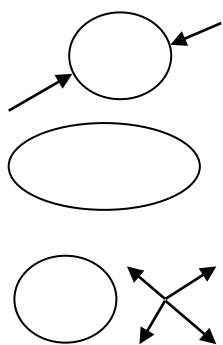


Figure 1.1: Production, growth, and removal of atmospheric aerosols (Source; Jacob,1999).

**The gas to particle conversion:** These particles originate from plant exhaust and combustion engines. They include soot, tar, sulfuric acid, etc. which are formed as follows: Through a chemical reaction catalyzed by ultra-violet radiation.



Through chemical reaction in small water droplets.



Clouds droplets absorb SO<sub>2</sub>.

A series of chemical reactions take place in the droplets

Particles consisting of sulfates and heavy metal left behind droplet evaporates

Figure 1.2: Aerosol formation (source: Cotton, 2000)

### **Formation of Aerosols by Mechanical and Chemical Disintegration at Solid Earth Surface.**

This process produces mainly large and giant particles.

Organic particles by plants and volcanic emissions Industrial particles injected from paper mills.

Mechanical and chemical disintegration of rocks, soils, and desert dust.

#### **1.1.2 Classification of Aerosol**

There are several classification schemes for atmospheric aerosols. Traditionally, aerosols are categorized into fine particles (diameter,  $D < 2.5 \mu\text{m}$ ) and coarse particles ( $D > 2.5 \mu\text{m}$ ). Haung (2010) further classified fine particles into Aitken (or nucleation) mode ( $0.001 - 0.1 \mu\text{m}$ ), accumulation mode ( $0.1 - 1 \mu\text{m}$ ). It can also be classified based on chemical compositions in the atmosphere such as sulphate (SF), sea salt (SS), soil dust (SD), black carbon (BC), and organic carbon (OC). Particles can also be geographically classified into maritime, continental, and background aerosols (Haung, 2010). These aerosol particles originate from a variety of natural and anthropogenic sources; they can be emitted in particulate form, or formed via gas-to-particle conversion under photolysis.

Table 1.1: Aerosol classification  $r$  = radius of the aerosol particles. (Source: Cotton, 2000)

<b>Classifications</b>	<b>Size</b>

Aitken particles	$r < 0.1\mu m$
Large particles	$0.1 \leq r \leq 1\mu m$
Giant particles	$r > 1.0\mu m$

**Formation of Aerosols by Mechanical and Chemical Disintegration at Solid Earth Surface.**

This process produces mainly large and giant particles.

Organic particles by plants and volcanic emissions Industrial particles injected from paper mills.

Mechanical and chemical disintegration of rocks, soils, and desert dust.

**1.1.3 Removal of Aerosol Particles from the Atmosphere**

Aerosols can be removed from the atmosphere through a lot of processes. The lifetime of any particular aerosol depends on its size and location. Larger aerosols settle out of the atmosphere very quickly under gravity, and some surfaces are more efficient at capturing aerosol than others. The various processes through which aerosols are removed are discussed below. The discussions are based on submissions of Cotton (2000).

**Wet deposition/ Scavenging**

Wet deposition is the name given to deposition pathways involving water. They include rainout, washout, sweep out. In rainout aerosol acts as nuclei for the condensation of cloud droplets. The aerosol (condensation nuclei) deposited in this way is said to have been rained out. It is a seasonal and latitudinal occurrence with 50% of aerosols that can be removed by rainouts (Jacobson, 2003). This implies most aerosols occurring in Nigeria and in particular the Niger

Delta can be rained out during the rainy season when the amount of water vapor and precipitation in the atmosphere is very high. Washout or scavenging occurs when falling precipitate coagulates with aerosol particles in the cloud, thereby bringing the aerosol to the surface. This is the removal of aerosol by cloud droplets.

**Sedimentation (Dry deposition)** - Dry deposition is a process of bringing aerosols to the surface without the aid of precipitation. They include:

**Gravitational Settling:** This is the process through which very large particles fall, reaching a terminal velocity. The fall speed is determined by a balance of gravity and the opposing drag force, the aerosol falls when the gravitational force outweighs the opposing drag force as shown in figure.1.3. The rate of fall of aerosol particles strongly depends on particle size and flow regimes.

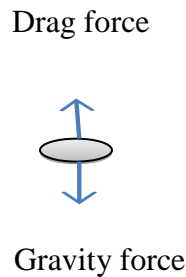


Figure 1.3: Drag force against gravity acting on an aerosol particle

The most important aerosol of atmospheric importance is within 0.1-1µm in diameter. The particles and their corresponding fall speed are as shown in table 1.2.

**Table 1.2: aerosol particle sizes and their fall speed (Source: Chin 2010)**

Diameter µm	Time to fall 1km	Diameter µm	Time to fall 1km

0.0005	9630 yr	4	23 days
0.02	230 yr	5	14.5 days
0.1	36 yr	10	3.6 days
0.5	3.2 yr	20	23 hrs
1	328 days	100	1.1 hrs
2	89 days	1000	4 mins
3	41 days	5000	1.8 mins

**Coagulation-** This is the process of removal of aerosols which involves the bumping and sticking together of aerosols particles in the size range of Aitken aerosol particles, thereby forming new particles whose sizes are large with a corresponding increase in fall speed.

#### **1.1.4 Effects of Aerosols on the Earth Systems**

Atmospheric aerosols play important role in the earth system and are one of the major uncertainties in climate change (IPCC, 2007). Aerosols influence air quality and public health, and climate by reflecting or absorbing sunlight, changing where and when clouds form. It has both direct and indirect effects on the atmosphere. The cooling or warming of the atmosphere due to the reflective or absorbent properties of the particles is considered direct effects (Haug, 2010). A reflective property of aerosol is such that the electromagnetic energy from the sun is scattered back into space while absorbent particles have the opposite effect thereby affecting the earth climate system (Boucher and Anderson,1995), and also impact on cloud and precipitation (Ramanathan., Crutzen., Kiehl.,, Rosenfeld 2001). According to the 2007 report of the Intergovernmental Panel on Climate Change (IPCC, 2007), the magnitude of the estimated radiative forcing of atmospheric aerosols is comparable with that of CO<sub>2</sub>, but with a cooling

effect and very large uncertainty. An indirect effect of aerosols is their roles as cloud condensation nuclei (CCN). Clouds with more CCN are larger are more reflective than those with fewer CCN, which in turn leads to the cooling of the atmosphere. Other radiative effects of atmospheric aerosols are as follows;

**Scattering of Radiation:** Radiation beam is scattered by particles in its path when its direction is altered without absorption taking place. Scattering can take place in the form of refraction, reflection, or diffraction of the radiation beam.

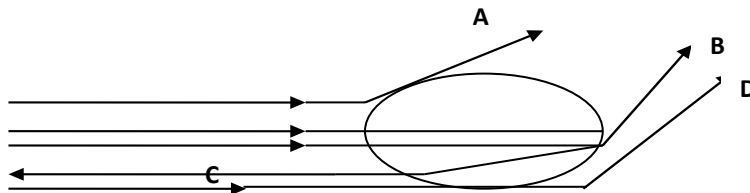


Figure 1.4: Scattering of solar radiation beam (A = refraction B=refraction C= internal reflection D=diffraction) (source: Cotton, 2000).

**Atmospheric Visibility Reduction:** Visibility is the ability of our eyes to extricate an object from the contiguous background. Solar radiation scattered by aerosol is responsible for the reduction in visibility in the troposphere, ordinarily, the human visibility range would have been 300km in the absence of aerosols (Cotton, 2000).

Besides these effects mentioned aerosols also have direct effects on health, acid deposition (acid rain), climate, and atmospheric chemistry.

## 1.2 Aim and Objectives

This study aims to characterize aerosol concentrations within the study area using satellite remote sensing data. The specific objectives of this study are:

- I) To identify and characterize aerosols to ascertain the dominant contaminants in the study area.

- II) To compare the dominant aerosols (CH<sub>4</sub>, CO, NO<sub>2</sub>, SO<sub>2</sub>) to ascertain their spatial/ temporal distribution, and
- III) To map the travel distance of aerosols using NOAA HYSPLIT data.

### **1.3 Statement of the problem**

Recently, there has been much progress in the understanding of aerosol sources, composition, reactions, and sinks, yet knowledge of the Spatio-temporal distribution of aerosol remains limited. In this work, the spatial distribution of aerosols will be investigated in detail to improve the representation of aerosol in climate models, and so to better understand their spatial distribution and size characteristics in some parts of the Niger Delta.

### **1.4 Justification of the study**

The need for the spatial mapping of aerosols cannot be over-emphasized. This spatial mapping and quantification have not been done in Niger Delta. This underscores the need for a proper study of the spatial distribution of atmospheric aerosols; hence, aerosols influence air quality, public health, and climate. Furthermore, the cost implication for the execution of this project is minimal because the data and software required are available at little or no cost.

### **1.5 Scope of the study**

In this study, satellite remote sensing was employed, which offers the advantage of providing the most extensive coverage in the shortest time interval. This allows for better tracking of the regional and global distribution of aerosols, in the extraction of aerosol properties which are extremely dynamic. The spatial coverage of this project will be areas under the Niger Delta.

## **CHAPTER TWO**

### **LITERATURE REVIEW**

#### **2.1 Review of related works**

Ayansina, Godwin & Margaret, (2019) in determining the effects of humidity, wind, and intertropical Discontinuity (ITD) movement on the seasonal distribution of atmospheric aerosols over different ecological zones in Nigeria, Satellite-observed aerosol optical depth (AOD), humidity, wind speed, and precipitation/ITD data were used. The datasets from Moderate Resolution Imaging Spectroradiometer (MODIS) AOD time series were used in this work. The wavelength of 550 nm MODIS AOD retrievals was also used and AOD data was re-scaled and

sub-divided into seasonal and annual distributions to investigate the variations in Aerosol. Kriging spatial interpolation models were also used to analyze the aerosol seasonal distribution. ITD Correlations analyses were used to evaluate the degree of influence of humidity, wind speed, and precipitation on the seasonal distribution of aerosol over six ecological zones; Sahel, Sudan, Guinea, Rainforest, Freshwater, and Mangrove zones in Nigeria. The results show that the AOD over Nigeria is influenced by meteorological factors, but much more influenced by dust sources outside the country. AOD appears much more during the Harmattan season than Wet and Dry seasons; with  $AOD \geq 0.46$ , with considerable concentration in Sahel ecological zone than other ecological zones. The results show a strong significant relationship between aerosol distribution and meteorological, principally humidity with  $R^2 \geq 0.65 @ p < 0.05$ . From the study, it was observed that daily variation of AOD, wind speed, humidity, and precipitation as well as the spatial distribution of dust sources in and outside the country are important drivers.

Barnabas, Samantha & Victor (2020) investigated the recording of Land Surface Temperature (LST) by Earth Observation (EO) Satellites for four gas flaring sites in Rivers State, Nigeria. Six Landsat 5 Thematic Mapper (TM) and Eleven Landsat 7 Enhanced Thematic Mapper Plus (ETM+) from 17 January 1986 to 08 March 2013 with  $< 5\%$  cloud contamination were considered. All the sites are located within a single Landsat scene (Path 188, Row 057). Dark Object Subtraction (DOS) method and Atmospheric Correction Parameter (ATMCORR) Calculator were used to obtain atmospheric correction effects parameters for multispectral and thermal bands [Upwelling radiance ( $L_u$ ), downwelling radiance ( $L_d$ ), and transmittance ( $\tau$ )] of Landsat data respectively. The emissivity ( $\epsilon$ ) for each site is estimated by using standard values for determining land surface cover from the Look-Up Table (LUT). The correction obtained from the DOS method was applied to the computed reflectance to get the atmospherically

corrected reflectance that was used for the classification of land cover. The  $L_u$ ,  $L_d$ , and  $\tau$  obtained were applied to the calibrated at-sensor radiance band 6 (high gain) data to compute the surface leaving radiance ( $L_\lambda$ ) with the  $\epsilon$  values obtained for each site. The Planck equation was inverted using the calibration constants to derive LST. Six ranges of LST values were retrieved for each flaring site, with Bonny Liquefied Natural Gas (LNG) Plant recorded the highest LST (345.0 K) and Umudioga Flow Station with the lowest (293.0 K). LST retrieved from both sensors for the flare hotspots are the highest values compared to other locations within the processing sites, which was clearly shown through Geospatial Information System (GIS) spatial analysis and the transects plots. Furthermore, the closer is the distance to the flare, the higher is the temperature and vice versa. Based on these results, it can be concluded that satellite-based sensors, such as Landsat TM and ETM+, can record LST at gas flaring sites in the Niger Delta.

Li, Dubovik, Derimian., Schuster, Lapyonok, Litvinov, ....., & Che,(2019) in this study presents a novel methodology for the remote monitoring of aerosol components over large spatial and temporal domains. The concept is realized within the GRASP (Generalized Retrieval of Aerosol and Surface Properties) algorithm to directly infer aerosol components from the measured radiances. The observed aerosols are assumed to be mixtures of hydrated soluble particles embedded with black carbon, brown carbon, iron oxide, and other (non-absorbing) insoluble inclusions. The complex refractive indices of the dry components are fixed a priori (although the refractive index of the soluble host is allowed to vary with hydration), and the complex refractive indices of the mixture are computed using mixing rules. The volume fractions of these components are derived along with the size distribution and the fraction of spherical particles, as well as the spectral surface reflectance in cases when the satellite data are inverted. The retrieval is implemented as a statistically optimized fit in a continuous space of solutions. This contrasts

with most conventional approaches in which the type of aerosol is either associated with a preassumed aerosol model that is included in a set of look-up tables or determined from the analysis of the retrieved aerosol optical parameters (e.g., single scattering albedo, refractive index, among others, provided by the AERONET retrieval algorithm); here, we retrieve the aerosol components explicitly. The approach also bridges directly to the quantities used in global chemical transport models. We first tested the approach with synthetic data to estimate the uncertainty, and then applied it to real ground-based AERONET and space-borne POLDER/PARASOL observations; thus, the study presents the first attempt to derive aerosol components from satellite observations specifically tied to the global chemical transport model quantities. Our results indicate aerosol optical characteristics that are highly consistent with standard products (e.g., R of  $\sim 0.9$  for aerosol optical thickness) and demonstrate an ability to separate intrinsic optical properties of fine- and coarse-sized aerosols. We applied our method to POLDER/PARASOL radiances on the global scale and obtained spatial and temporal patterns of the aerosol components that agree well with existing knowledge on aerosol sources and transport features. Finally, we discuss the limitations and perspectives of this new technique.

Bhaga, Trisha., Dube, Timothy, Shoko & Cletah. (2020) in climate variability and recurrent droughts have caused remarkable strain on water resources in most regions across the globe, with the arid and semi-arid areas being the hardest hit. The impacts have been notable on surface water resources, which are already under threat from massive abstractions due to increased demand, as well as poor conservation and unsustainable land management practices. Drought and climate variability, as well as their associated impacts on water resources, have gained increased attention in recent decades as nations seek to enhance mitigation and adaptation mechanisms. Although the use of satellite technologies has, of late, gained prominence in generating timely

and spatially explicit information on drought and climate variability impacts across different regions, they are somewhat hampered by difficulties in detecting drought evolution due to its complex nature, varying scales, the magnitude of its occurrence, and inherent data gaps. Currently, some studies have been conducted to monitor and assess the impacts of climate variability and droughts on water resources in sub-Saharan Africa using different remotely sensed and in-situ datasets. This study, therefore, provides a detailed overview of the progress made in tracking droughts using remote sensing, including its relevance in monitoring climate variability and hydrological drought impacts on surface water resources in sub-Saharan Africa. The paper further discusses traditional and remote sensing methods of monitoring climate variability, hydrological drought, and water resources, tracking their application and key challenges, with a particular emphasis on sub-Saharan Africa. Additionally, characteristics and limitations of various remote sensors, as well as drought and surface water indices, namely, the Standardized Precipitation Index (SPI), Palmer Drought Severity Index (PDSI), Normalized Difference Vegetation (NDVI), Vegetation Condition Index (VCI), and Water Requirement Satisfaction Index (WRSI), Normalized Difference Water Index (NDWI), Modified Normalized Difference Water Index (MNDWI), Land Surface Water Index (LSWI+5), Modified Normalized Difference Water Index (MNDWI+5), Automated Water Extraction Index (shadow) (AWEIsh), and Automated Water Extraction Index (non-shadow) (AWEInsh), and their relevance in climate variability and drought monitoring are discussed. Additionally, key scientific research strides and knowledge gaps for further investigations are highlighted. While progress has been made in advancing the application of remote sensing in water resources, this review indicates the need for further studies on assessing drought and climate variability impacts on water resources, especially in the context of climate change and increased water demand. The results from this

study suggest that Landsat-8 and Sentinel-2 satellite data are likely to be best suited to monitor climate variability, hydrological drought, and surface water bodies, due to their availability at relatively low cost, impressive spectral, spatial, and temporal characteristics. The most effective drought and water indices are SPI, PDSI, NDVI, VCI, NDWI, MNDWI, MNDWI+5, AWEIsh, and AWEInsh. Overall, the findings of this study emphasize the increasing role and potential of remote sensing in generating spatially explicit information on drought and climate variability impacts on surface water resources. However, there is a need for future studies to consider spatial data integration techniques, radar data, precipitation, cloud computing, and machine learning or artificial intelligence (AI) techniques to improve on understanding climate and drought impacts on water resources across various scales.

To better understand the aerosol properties over the Arctic, Antarctic, and Tibetan Plateau (TP), Yang, Y., Zhao, C., Wang, Q., Cong, Z., Yang, X., & Fan, H(2021) investigated the aerosol optical properties using 13 years of CALIPSO (Cloud-Aerosol Lidar and Infrared Pathfinder Satellite Observations) L3 data. The back trajectories for air masses were also simulated using the Hybrid Single-Particle Lagrangian Integrated Trajectory (HYSPLIT) model. The results show that the aerosol optical depth (AOD) has obvious spatial- and seasonal variation characteristics, and the aerosol loading over Eurasia, Ross Sea, and South Asia is relatively large. The annual average AODs over the Arctic, Antarctic, and TP are 0.046, 0.024, and 0.098, respectively. Seasonally, the AOD values are larger from late autumn to early spring in the Arctic, in winter and spring in the Antarctic, and spring and summer over the TP. There are no significant temporal trends of AOD anomalies in the three study regions. Clean marine and dust-related aerosols are the dominant types over ocean and land, respectively, in both the Arctic and Antarctic, while dust-related aerosol types have greater occurrence frequency (OF) over the TP.

The OF of dust-related and elevated smoke is large for a broad range of heights, indicating that they are likely transported aerosols, while other types of aerosols mainly occurred at heights below 2 km in the Antarctic and Arctic. The maximum OF of dust-related aerosols mainly occurs at 6 km altitude over the TP. The analysis of back trajectories of the air masses shows large differences among different regions and seasons. The Arctic region is more vulnerable to mid-latitude pollutants than the Antarctic region, especially in winter and spring, while the air masses in the TP are mainly from the Iranian Plateau, Tarim Basin, and South Asia.

Uchi (2021) in his study assessed dust haze over northern Nigeria. Data on dust haze, rainfall, and wind speed were acquired at Nigerian Meteorological Agency (NIMET), Oshodi, Lagos, for thirty years (1988-2017). The data were collected from sixteen synoptic stations, namely Abuja, Bauchi Bida, Gusau, Jos, Kaduna, Kano, Katsina, Maiduguri, Minna, Nguru, Potiskum, Sokoto, Yelwa, Yola, and Zaria. The data were analyzed using mean, standard deviation, and coefficient of variation (CV). The least-square regression model was employed to determine the trend in the temporal variation of dust haze in the study area. Graphs, isocline, and choropleth maps were used to analyze spatial variation in Thick Dust Haze (TDH). The result of the average monthly concentration of dust haze indicates that the highest average monthly parts per million (ppm) usually occurred in December and this then followed by January, while the lowest concentration occurred in August and July. The result also revealed that there is an increasing trend only for Gusau, Potiskum, Maiduguri, Zaria, Kaduna, Abuja, Yola, and Bida. However, only the trend of Abuja and Yola was significant. A significant decreasing trend of the dust haze phenomenon was observed at Sokoto, Nguru, Kano, Katsina, Yelwa, Bauchi, Jos, and Minna. However, these coefficients were not significant at 0.05 confidence level using student's test statistics. The trend in annual variation indicates a downward trend during the study period. The result further

showed that the spatial variation in dust haze decreases southward from a drier north to the wetter southern part of northern Nigeria. This is attributed to the proximity to the Sahara desert, wind direction, and topography.

Daful.,Adewuyi,.,Dadan-Garba,.,Oluwole, Muhammad &, Ezeamaka,(2020) in their study appraised the local and global implication of ambient air quality index of Kaduna Metropolis, Nigeria. With the point of investigating the spatial and transient dissemination of the Air Quality Index (AQI) of Carbon monoxide (CO), Sulphur dioxide (SO<sub>2</sub>), and Particulate Matter (PM<sub>10</sub>) and their suggestions on human wellbeing, given neighborhood and global measures. Data were collected during the rainy season and dry harmattan weather. From traffic, Industrial, commercial and residential areas, utilizing validated portable pollutant monitors (MSA Altair 5x Gas Detector) to collect data on the concentration of air pollutants (CO and SO<sub>2</sub>) and (CWHAT200 Particulate Counter) for the concentration of particulate matters (PM<sub>10</sub>). Equal allocation stratifies sampling and purposive sampling was utilized for the selection of sample points. The data were analyzed in line with the USEPA Air Quality Index calculation approach and using descriptive statistics. The findings reveal that the AQI of Kaduna Metropolis ranges from good to hazardous, CO has 57.57% and 24.24% of the sample sites AQI ranging from unhealthy to hazardous based on WHO/USEPA and NESREA standards respectively. Equally, SO<sub>2</sub> has about 91%, 34.23%, 42.42% of the sites while AQI ranged from unhealthy to hazardous based on WHO, USEPA, and NESREA standards respectively. PM<sub>10</sub> has 75.76% and 18.18% of the sites while AQI was revealed as hazardous based on WHO and USEPA standards, whereas none of the sites AQI is hazardous base on the NESREA standard. Further analysis shows that the northern part of the metropolis has more sites with unhealthy AQI than the southern part of the metropolis. Also, the traffic land use has more of its sites AQI ranging from unhealthy to

Sensitive group to hazardous. In conclusion, this study provides empirical data on the AQI of Kaduna metropolis which ranges from good to hazardous. Thus, the need for enforcement agencies to strictly enforce the guidelines regulating ambient pollution in the study area.

Adimula, Falaiye & Adindu (2008) used AERONET AOD and NIMET visibility data to show that coarse aerosols are the major class of aerosol responsible for persistent visibility reduction over the years.

Chiemeka, Oleka & Chineke (2009), used Atomic Absorption Spectroscopy (AAS) to analyze dust samples collected at Uturu during the Harmattan to determine the mass concentrations of aerosols in air, mean aerosol sizes, and the elemental concentrations of aerosols.

Nwofor (2010), used AERONET Aerosol Optical Depth (AOD) and Angstrom Exponent data of Ilorin from (1998-2008) to show that between 1998 & 2003 the dust in the atmosphere originates from Sahara while between 2004 & 2008 dust observed all year round was due to local dust pollution which was as a result of persistent long-term drought and resulting aridity of Ilorin.

Obiajunwa, Johnson-Fatokun, Olaniyi, & Olowole (2002). used samples collected with Whatman filters and analyzed using the Energy-dispersive X-ray fluorescence technique to determine the elemental concentration of aerosol within a factory site with the TSP values ranging from 70 to 7963  $\mu\text{g}/\text{m}^3$ , the annual average set by the national regulatory agency, FEPA, by factors ranging from 2 to 32 times.

Oluleye, Ogunjobi, Bernard, Ajayi & Akinsanola (2012) using Satellite and AERONET data (2005-2009) for Sahelian West Africa concluded that aerosol optical depth showed large variation with high values recorded during the harmattan dry months and low values during the rain/monsoon season.

Oyem and Igbafe, (2010) studied the transport patterns of aerosol over Nigeria using HYSPLIT and meteorological data to show that precipitation, wind speed, and relative humidity alter the aerosol loading at different times of the year maintaining an inverse relationship.

Anuforom, Akeh, Okeke & Opara, (2007) used total ozone mapping spectrometer aerosol index (TOMS AI) and horizontal visibility data from synoptic stations for the Sahelian parts of Nigeria to show that visibility had been on the decrease over the period as a result of increased episodic dust events in Nigeria during the Harmattan. He further showed that AI correlates strongly with visibility data.

Oyediran Owoade, Fawole, Olise, Ogundele, Hezekiah & Hopke (2013) Size segregated suspended particulate matter (PM<sub>2.5</sub> and PM<sub>2.5-10</sub>) were collected using Gent low-volume air sampler at four different receptor site-classes in Lagos Mega City, Nigeria. The particulate mass loading was quantified and the concentration was analyzed to examine the pattern and variation from one receptor site-class to another. The PM<sub>2.5</sub>/PM<sub>10</sub> ratio varied among the site classes with the residential and marine sites having the least and highest ratio of  $0.31 \pm 0.13$  and  $0.49 \pm 0.17$  respectively. Particulate loading was higher on weekdays than on weekends (by a factor of about 1.5) in all but the marine site class. The mean PM<sub>2.5</sub>/PM<sub>10</sub> ratio is  $0.41 \pm 0.15$ , which suggests that traffic emission is not the principal source of the Particulate Matter (PM). The INAA assay of the particulates detected ten elements: As, Br, Ce, K, La, Mo, Na, Sb, Sm, and Zn. Except for Br, Mo, and Sb, the detected elements were more pronounced in the coarse fractioned filter. Principal Component Factor Analysis (PCFA) of the detected elements identified some common sources (traffic-related, traffic emission, sea-salt, and industrial emission) for both PM fractions at the four receptor site classes.

Despite the extensive work done by these authors none of them considered studying the impact of atmospheric aerosols in Oil exploration areas in the Niger Delta as the whole judging by its geographical and industrial differences.

Secondly, most of these studies made use of in-situ data which are limited in spatial coverage to undertake their studies. Therefore, in this study we used a combination of various data sources (AIRS, OMI data's) from remote sensing satellites using models to identify, map, characterize and apportion atmospheric aerosols.

## **2.2 Remote Sensing**

The subject of remote sensing is as old as man, but what has been evolving are the remote sensing platforms themselves. According to the definition by Lillesand, Kiefer & Chipman, (2008), remote sensing is the science and art of obtaining information about an object, area, or phenomenon through the analysis of data acquired by a device that is not in contact with the object, area or phenomenon under investigation. This definition underscores the fact that man had been using a lot of remote sensing platforms in the time past. Such ways are from space, ground, balloons, spacecraft, etc. This depends on the depth of the atmosphere being investigated, hence in each platform certain parameters with specific characteristics are measured. Examples are ground-level measurements of aerosols and rainfall made with simple sun-photometer and rain gauge etc. Through the depth of the troposphere, balloon-borne instruments (radiosondes) are used, such that they transmit information back to the surface by radio e.g humidity and temperatures. At higher altitudes, research balloons and aircraft can be used to measure air samples in the lower stratosphere and rockets can measure meteorological activities in the mesosphere and beyond. A perfect example is an aerial photograph which usually makes use of a camera alongside a film. The sun is a source of energy or radiation, which

provides a very convenient source of energy for remote sensing. The sun's energy is either reflected, as it is for visible wavelengths, or absorbed and then reemitted, as it is for thermal infrared wavelengths. Aerial photography in the visible portion of the electromagnetic wavelength was the original form of remote sensing but technological developments have enabled the acquisition of information at other wavelengths including near-infrared, thermal infrared, and microwave. The collection of information over a large number of wavelength bands is referred to as multispectral or hyperspectral data. The development and deployment of manned and unmanned satellites have enhanced the collection of remotely sensed data and offer an inexpensive way to obtain information over large areas. The capacity of remote sensing to identify and monitor land surfaces and environmental conditions has expanded greatly over the last few years and remotely sensed data will be an essential tool in natural resource management. Remote sensing involves the measurement of energy in many parts of the electromagnetic (EM) spectrum. The major regions of interest in satellite sensing are visible light, reflected and emitted infrared, and microwave regions. The measurement of this radiation takes place in what is known as spectral bands. Remote sensing makes use of visible, near-infrared, and short-wave infrared sensors to form images of the earth's surface by detecting the solar radiation reflected from targets on the ground. Different materials reflect and absorb differently at different wavelengths. This, the targets can be differentiated by their spectral reflectance signatures in the remotely sensed images. In remote sensing, a detector measures the electromagnetic (EM) radiation that is reflected from the earth's surface materials. These measurements can help to distinguish the type of land covering. Soil, water, and vegetation have different patterns of reflectance and absorption over different wavelengths. These platforms already mentioned are classified as in-situ measurements. On the other hand, rather than taking measurements in the vicinity of the

measuring apparatus, one can implore the use of remote sensing. Remote sensing measurements employ the use of the principle of electromagnetic radiation which is scattered, absorbed, emitted, or transmitted radiation by the atmosphere.

$$I = \left(\frac{E_R}{E_I}\right)_\lambda + \left(\frac{E_T}{E_I}\right)_\lambda + \left(\frac{E_E}{E_I}\right)_\lambda + \left(\frac{E_S}{E_I}\right)_\lambda \quad (2.1)$$

I = Intensity, ER = Reflection Energy,  $\lambda$  = Wavelength

ET = Transmission Energy, EE = Emission Energy

EI = Incidence Energy, ES = Scattering Energy

Remote sensing is categorically divided into, active and passive remote sensing. Passive remote sensing techniques employ the use of external sources of energy, for illumination. Passive sensor systems are based on the reflection of solar energy from the Sun, which makes them active only during daylight (Woldai, 2002). For active remote sensing, an internal source of energy is used to direct radiation into the atmosphere where they are reflected, either scattered, absorbed, or transmitted by atmospheric molecules, aerosols, or inhomogeneity of atmospheric structure which are then detected by a receiver.

### **2.2.1 Atmospheric Satellite Remote Sensing**

Earth-orbiting satellites provide enormous possibilities for global-scale measurements of the atmosphere from space (Andrews, 2000). The Earth-orbiting satellites take a lot of measurements depending on the designed measurement characteristics of the sensor. Such measurements are aerosols, temperature, precipitation, and other meteorological and environmental characteristics. Examples are the geostationary satellites which orbit the earth at 36000km above the equator and monitor weather and other meteorological parameters. Polar-orbiting and other non-geostationary satellites orbits between 700-1000km above sea level. They measure temperature and atmospheric compositions at vertical levels. Therefore, in this study, we made use of non-

geostationary satellites of OMI, AIRS, TOMS, and NOAA HYSPLIT to measure aerosol loading in the areas of study under the Niger Delta. Satellites extracting information about aerosols make use of the passive remote sensing techniques. The sensors measure top of the atmosphere (TOA) radiance in an event of a cloud-free atmosphere, aerosols scatter, reflect, and/or absorbs radiance (Veefkind & Lercher, 1999). This is based on the fact that the light beam passing through the atmosphere is attenuated by aerosols and atmospheric gas particles, the mathematical expression is given by Beer-Lambert's law written as:

$$\frac{I_{\lambda}}{I_{\lambda,0}} = e^{-\sigma_{e,\lambda}L} \quad (2.2)$$

where  $I_{\lambda}$  ( $\text{Wm}^{-2}$ ) and  $I_{\lambda,0}$  ( $\text{Wm}^{-2}$ ) are the light intensities at wavelength  $\lambda,0$  incident on the column and at a distance L, respectively. Satellite aerosol measurement is an optical technique for detecting the light scattered by atmospheric aerosols. Based on the radiative signal at the top of the atmosphere, certain integral properties and a Spatio-temporal pattern of atmospheric aerosols are inferred. Satellite aerosol observations are the only available techniques to measure the distribution of aerosol over the entire globe simultaneously. Satellite-based measurement of atmospheric aerosol properties has inherent physical and mathematical limitations that are yet to be fully understood and the tools and methods are still maturing. Generally, the art and science of satellite aerosol remote sensing consist of combining the knowledge and insights from the complementary research areas of atmospheric aerosols and of remote sensing (Husar, 2006).

The Total Monitoring Spectrometer (TOMS) and Ozone Monitoring Imaging (OMI) were used to provide better estimates of atmospheric pollutants and their transport through the Earth's atmosphere (Liu & Hong, 2012). The parameters of interest acquired by this sensor are  $\text{NO}_2$  and  $\text{SO}_2$ . The Atmospheric Infrared Sounder (AIRS) was used to retrieve CO and  $\text{CH}_4$ .

The Hybrid Single-Particle Lagrangian Integrated Trajectory (HYSPLIT) model was used to determine the origin and speed of air masses, in other to assess the influence that long-distance transport from various parts in the area of study have on the aerosol loading in line with (Draxler & Hess, 1998).

All the data retrieved for this research spans from 2013-2015 which gave a two (2) year interval. Further discussions on these instruments and models are given in the sub-sections below.

### **2.2.2 Scattering of Radiation**

A radiation beam is scattered by a particle in its path when its direction of propagation is deviated without absorption taking place. This may be in the form of reflection, refraction, or diffraction of the beam (light). When light is scattered, it implies that its direction of movement has been altered, hence it will follow a different course altogether. This perturbation depending on the property of the aerosol involved will have a direct or indirect effect, such as visibility reduction (Cotton, 2000), and cooling of the earth as was the case during the volcanic eruption of Mount Pinatubo in 1991 (Jacob, 1999). This gives rise to the creation of the phenomenon called aerosols optical depth (AOD/ AOT) in the case of aerosol measurement.

### **2.2.3 Characterization of Aerosols**

Smoke from biomass burning and dust particles from desert storms are among the main atmospheric constituents that affect the air quality and the Earth's climate system. Monitoring of these atmospheric constituents is possible through satellite measurements as well as ground measurements. But ground measurements are very limited in space and time because these constituents can be transported far away from their source (Liu *et al.*, 2012). In this research, we used a combination of OMI and AIRS to characterize aerosols.

#### **2.2.4 Scattering and Absorption of light by Aerosol**

The attenuation of solar radiation by aerosols has several important influences on the atmosphere and the ecological environment. Aerosols reduce visibility and alter climate through the scattering and absorption of solar radiation (Charlson, Schwartz, Hales, Cess, Coakley, Hansen, & Hofmann, 1992). They impact photochemistry thereby forming stratospheric ozone, through the modification of atmospheric energy balance. They also influence crop production by the attenuation of the Photosynthetically Active Radiation (PAR). The direct influence of aerosols on climate as well as crop production depends on several factors which are aerosol optical depth (AOD), aerosol single scattering albedo (ASSA), and the aerosol up scatter fraction (SF). The relationship between light attenuation and the scattering and absorption by aerosols is given by Beer-Lambert's law given in equation 2.2.

#### **2.2.5 Advantages of In-situ measurements**

- It may give an accurate reading.
- Higher-resolution measurement.
- Provide data with high vertical resolution.

#### **2.2.6 Disadvantages In-situ measurements**

- Samples a small area.
- Measure in an unrepresentative of the regions.
- Need human monitoring for hardware maintenance and to guard against theft.

#### **2.2.7 Advantages of remote sensing from Satellites**

- Can give near-global coverage.
- Adds value when combined with surface monitors and models
- Provides coverage where ground monitors are almost impossible

- Synoptic and transboundary view (time and space), visual context is more appealing to the eyes.
- Qualitative assessments and indications of the long-range transport
- Emerging Application areas

### **2.2.8 Disadvantages remote sensing from Satellites**

- Satellites are expensive to put in space.
- They are difficult to repair when they spoil.
- It has a lower resolution compared to in-situ measurements.
- Processing the data needs a lot of expertise and techniques.
- Results need to be validated.

Generally, a blend of the two observational technologies gives near-perfect information about the prevailing situation within the environment.

### **2.3.1 Oil Spill/Gas Flaring**

The key environmental issues in the Niger Delta of Nigeria relate to its petroleum industry. The delta covers 20,000km<sup>2</sup> within wetlands of 70,000km<sup>2</sup> formed primarily by sediment deposition. Home to 20 million people and 40 different ethnic groups, this floodplain makes up 7.5% of Nigeria's total landmass. It is the largest drainage basin in Africa. The delta's environment can be broken down into four ecological zones: coastal barrier islands, mangrove swamp forests, freshwater swamps, and lowland rainforests. This incredibly well-endowed ecosystem contains one of the highest concentrations of biodiversity on the planet. The region could experience a loss of 40% of its inhabitable terrain in the next thirty years as a result of extensive dam construction in the region. The carelessness of the oil industry has also precipitated this situation, which can perhaps be best encapsulated by a 1983 report issued by the NNPC, long before

popular unrest surfaced. We witnessed the slow poisoning of the waters of this country and the destruction of vegetation and agricultural land by oil spills that occur during petroleum operations. But since the inception of the oil industry in Nigeria, more than twenty-five years ago, there has been no concerned and effective effort on the part of the government, let alone the oil operators, to control environmental problems associated with the industry.

### **2.3.2 Extent of the problem**

Reports on the extent of the oil spills vary. The Department of Petroleum Resources estimated 1.89 million barrels of petroleum were spilled into the Niger Delta between 1976 and 1996 out of the total of 2.4 million barrels spilled in 4,835 incidences (220,000 cubic metres). A UNDP report states that there have been a total of 6,817 oil spills between 1976 and 2001, which accounts for a loss of 3 million barrels of oil of which more than 70% was not recovered. 69% of these spills occurred offshore, a quarter was in swamps and 6% spilled on land. The NNPC places the quantity of petroleum jettisoned into the environment yearly at 2,300 cubic metres with an average of 300 individual spills annually. However, because these amounts do account for "minor" spills, the World Bank argues that the true quantity of petroleum spilled into the environment could be as much as 10 times the officially claimed amount. The largest individual spills include the blowout of a Texaco offshore station which in 1980 dumped an estimated 400,000 barrels (64,000 metre cubic) of crude oil into the Gulf of Guinea and Royal Dutch Shell's Forcados terminal tank failure which produced a spillage estimated at 580,000 barrels (92,000 metre cube). Baird reported that between 9 million and 13 million barrels have been spilled in the Niger Delta since 1958.

### **2.3.3 Causes**

Oil spills are a common event in Nigeria. Half of all spills occur due to pipeline and tanker accidents (50%), other causes include sabotage (28%) and oil production operations (21%), with 1% of the spills being accounted for by inadequate or non-functional production equipment. Corrosion of pipelines and tankers is the rupturing or leaking of old, production infrastructures that often do not receive inspection and maintenance. A reason that corrosion accounts for such a high percentage of all spills is that as a result of the small size of the oilfields in the Niger Delta, there is an extensive network of pipelines between the fields, as well as numerous small networks of flow lines the narrow diameter pipes that carry oil from wellheads to flow stations allowing many opportunities for leaks. In onshore areas, most pipelines and flow lines are laid above ground. Pipelines, which have an estimated life span of about fifteen years, are old and susceptible to corrosion. Sabotage is performed primarily through what is known as "bunkering", whereby the saboteur attempts to tap the pipeline. In the process of extraction sometimes, the pipeline is damaged or destroyed. Oil extracted in this manner can be sold. Sabotage and theft through oil siphoning have become a major issue in the Niger Delta states as well, contributing to further degradation.

### **2.3.4 Consequences**

Oil spillage has a major impact on the ecosystem into which it is released and constitutes ecocide. Immense tracts of the mangrove forests, which are especially susceptible to oil (mainly because it is stored in the soil and re-released annually during inundations), have been destroyed. Spills in populated areas often spread out over a wide area, destroying crops and aquacultures through contamination of groundwater and soils. The consumption of dissolved oxygen by bacteria feeding on the spilled hydrocarbons also contributes to the death of fish. Because of the

careless nature of oil operations in the delta, the environment is growing increasingly uninhabitable.

### **2.3.5 Gas Flaring in Nigeria**

Nigeria flares 17.2 billion m<sup>3</sup> of natural gas per year in conjunction with the exploration of crude oil in the Niger Delta. This high level of gas flaring is equal to approximately one-quarter of the current power consumption of the African continent. Even though we have grown to be fairly dependent on oil and it has become the centre of current industrial development and economic activities, we rarely consider how oil exploration and exploitation processes create environmental health and social problems in local communities near oil-producing fields. The environment and human health have frequently been secondary considerations for oil companies and the Nigerian government. However, although there may be reasons for the continuous gas flaring, many strong arguments are suggesting that it should be stopped. because of this massive oil exploration in the Niger Delta, the ramifications for human health, local culture, indigenous self-determination, and the environment are severe. A gas flare, alternatively known as a flare stack, is a gas combustion device used in industrial plants such as petroleum refineries, chemical plants, natural gas processing plants as well as at oil or gas production sites having oil wells, gas wells, offshore oil and gas rigs, and landfills. In industrial plants, flare stacks are primarily used for burning off flammable gas released by pressure relief valves during unplanned over-pressuring plant equipment. During plant or partial plant startups and shutdowns, flare stacks are also often used for the planned combustion of gases over relatively short periods.



Figure 2.1: Images of Gas Flaring in Niger Delta

### **2.3.6 Environmental Implication**

#### **2.3.6a Climate Change**

Gas flaring contributes to climate change, which has serious implications for both Nigeria and the rest of the world. The burning of fossil fuels, mainly coal, oil, and gas greenhouse gases, has led to warming up the world and is projected to get much worse during the 21st century. According to the intergovernmental panel on climate change (IPCC). Climate change is particularly serious for developing countries and Africa as a continent is regarded as highly vulnerable with limited ability to adapt. Gas flaring contributes to climate change by the emission of carbon dioxide, the main greenhouse gas. Venting of the gas without burning, a practice for which flaring seems to be treated as a synonym releases methane the second main

greenhouse gas together and crudely, these gases make up about eighty percent of global warming to date.

### **2.3.6b Acid Rain**

Acid rain has been linked to the activities of gas flaring. Corrugated roofs in the delta region have been corroded by the composition of the rain that falls as a result of flaring. The primary causes of acid rain are sulphur dioxide (SO<sub>2</sub>) and nitrogen oxide (NO) which combine with atmospheric moisture to form sulphuric acid and nitric acid respectively. Size and environmental philosophy in the industry have a very strong positive impact on the gas flaring-related CO<sub>2</sub>. Acid rain acidifies lakes and streams and damages vegetation. In addition, acid rain accelerates the decay of building materials and paints. Before falling to the earth, SO<sub>2</sub> and NO<sub>2</sub> gases and their particulate matter derivatives, sulphates, and nitrates, contribute to visibility degradation and harm public health.

### **2.3.6c Agriculture**

The flares associated with gas flaring give rise to the atmospheric contaminant. This includes oxides of nitrogen, carbon, sulphur (NO<sub>2</sub>, CO<sub>2</sub>, CO, and SO<sub>2</sub>), particulate matter, hydrocarbon and ash, photochemical oxidants, and hydrogen sulphide (H<sub>2</sub>S). These contaminants acidify the soil, hence depleting soil nutrients. previous studies have shown that the nutritional values of crops within such vicinity are reduced. In some cases, there is no vegetation in the areas surrounding the flare due partly to the tremendous heat that is produced and the acid nature of soil P<sup>H</sup>.

The effects of the changes in temperature on crops included stunted growth, scotched plants, and such other effects as withered young crops. Reference concluded that the soils of the study area

are fast losing their fertility and capacity for sustainable agriculture due to the acidification of the soils by the various pollutants associated with gas flaring in the area.

### **2.3.7 Health Implications**

#### **2.3.7a Adverse Effects**

The implication of gas flaring on human health is all related to the exposure of those hazardous air pollutants emitted during incomplete combustion of gas flare. These pollutants are associated with a variety of adverse health impacts, including cancer, neurological, reproductive, and developmental effects. Deformities in children, lung damage, and skin problem have also been reported.

#### **2.3.7b Haematological Effects**

Hydrocarbon compounds are known to cause some adverse changes in hematological parameters. These changes affect blood and blood-forming cells negatively. And could give rise to anaemia (aplastic), pancytopenia, and leukaemia.

#### **2.3.7c Economic Loss**

Aside from the health and environmental consequences of gas flaring, the nation also loses billions of dollars worth of gas which is burnt off daily in the atmosphere. Much of this can be converted for domestic use and electricity generation. By so doing the level of electricity generation in the country could be raised to meet national demand. Nigeria has recorded a huge revenue loss due to gas flaring and oil spillage. Though more than 65% of government revenue is from oil.

#### **2.3.7d Pollution**

Drilling mud and oil sometimes find their way to the streams, surface waters, and land thus making them unfit for consumption nor habitable by man or animal. This problem has been

produced by a range of international oil companies which have been in operation for over four decades. The economic ramifications of this high level of gas flaring are serious because this process is a significant waste of potential fuel which is simultaneously polluting water, air, and soil in the Niger Delta.

### **2.3.8 Impacts of waste flaring associated gas from oil drilling sites**

Improperly operated flares may emit methane and other volatile organic compounds as well as sulphur dioxide and other sulphur compounds, which are known to exacerbate asthma and other respiratory problems. Other emissions from improperly operated flares may include, aromatic hydrocarbons (benzene, toluene, xylenes) and benzopyrene, which are known to be carcinogenic. The amount of flaring and burning of associated gas from oil drilling sites is a significant source of carbon dioxide (CO<sub>2</sub>) emissions. Coupled with fossil fuel combustion and cement production, flaring's carbon dioxide emissions in 2010 have tripled (1300 + 110 GtCO<sub>2</sub>) compared to the last recording (years 1750-1970, 420 + 35 GtCO<sub>2</sub> had been emitted). 2400 x 10<sup>6</sup> tons of carbon dioxide are emitted annually in this way and it amounts to about 1.2 percent of the worldwide emissions of carbon dioxide.

### **2.4 Climate Change**

Climate change in IPCC usage refers to a change in the state of the climate that can be identified (e.g. using statistical tests) by changes in the mean and/or the variability of its properties, and that persists for an extended period, typically decades or longer. It refers to any change in climate over time, whether due to natural variability or as a result of human activity. This usage differs from that in the United Nations Framework Convention on Climate Change (UNFCCC), where climate change refers to a change of climate that is attributed directly or indirectly to human

activity that alters the composition of the global atmosphere and that is in addition to natural climate variability observed over comparable periods (IPCC, 2007).

#### **2.4.1 Global Carbon Cycle Overview**

Atmospheric CO<sub>2</sub> represents the main atmospheric phase of the global carbon cycle. The global carbon cycle can be viewed as a series of reservoirs of carbon in the Earth System, which is connected by exchange fluxes of carbon. Conceptually, one can distinguish two domains in the global carbon cycle. The first is a fast domain with large exchange fluxes and relatively 'rapid' reservoir turnovers, which consists of carbon in the atmosphere, the ocean, surface ocean sediments, and on land in vegetation, soils, and freshwaters. Reservoir turnover times, defined as reservoir mass of carbon divided by the exchange flux, ranging from a few years for the atmosphere to decades to millennia for the major carbon reservoirs of the land vegetation and soil and the various domains in the ocean. A second, slow domain consists of the huge carbon stores in rocks and sediments which exchange carbon with the fast domain through volcanic emissions of CO<sub>2</sub>, chemical weathering, erosion, and sediment formation on the seafloor. Turnover times of the (mainly geological) reservoirs of the slow domain are 10,000 years or longer. Natural exchange fluxes between the slow and the fast domain of the carbon cycle are relatively small (<0.3 PgC yr<sup>-1</sup>, 1 PgC = 10<sup>15</sup> gC) and can be assumed as approximately constant in time (volcanism, sedimentation) over the last few centuries, although erosion and river fluxes may have been modified by human-induced changes in land use.

During the Holocene (beginning 11,700 years ago) before the Industrial Era, the fast domain was close to a steady-state, as evidenced by the relatively small variations of atmospheric CO<sub>2</sub> recorded in ice cores, despite small emissions from human-caused changes in land use over the last millennia (Pongratz *et al.*, 2009). By contrast, since the beginning of the Industrial Era, fossil

fuel extraction from geological reservoirs, and their combustion, has resulted in the transfer of the significant amount of fossil carbon from the slow domain into the fast domain, thus causing an unprecedented, major human-induced perturbation in the carbon cycle. In the atmosphere, CO<sub>2</sub> is the dominant carbon-bearing trace gas with a current (2011) concentration of approximately 390.5 ppm, which corresponds to a mass of 828 PgC (Prather *et al.*, 2012). Additional trace gases include methane (CH<sub>4</sub>, current content mass ~3.7 PgC) and carbon monoxide (CO, current content mass ~0.2 PgC), and still smaller amounts of hydrocarbons, black carbon aerosols, and organic compounds. The terrestrial biosphere reservoir contains carbon in organic compounds in vegetation living biomass (450 to 650 PgC; Prentice *et al.*, 2001) and dead organic matter in litter and soils (1500 to 2400 PgC; Batjes, 1996). There is an additional amount of old soil carbon in wetland soils (300 to 700 PgC; Bridgham *et al.*, 2006) and in permafrost soils (~1700 PgC; Tarnocai *et al.*, 2009); albeit some overlap with these two quantities. CO<sub>2</sub> is removed from the atmosphere by plant photosynthesis (Gross Primary Production (GPP), 123±8 PgC yr<sup>-1</sup>, (Beer *et al.*, 2010), and carbon fixed into plants is then cycled through plant tissues, litter, and soil carbon and can be released back into the atmosphere by autotrophic (plant) and heterotrophic (soil microbial and animal) respiration and additional disturbance processes (e.g., sporadic fires) on a very wide range of time scales (seconds to millennia). Because CO<sub>2</sub> uptake by photosynthesis occurs only during the growing season, whereas CO<sub>2</sub> release by respiration occurs nearly year-round.

The carbon cycle is as shown in the figure below:

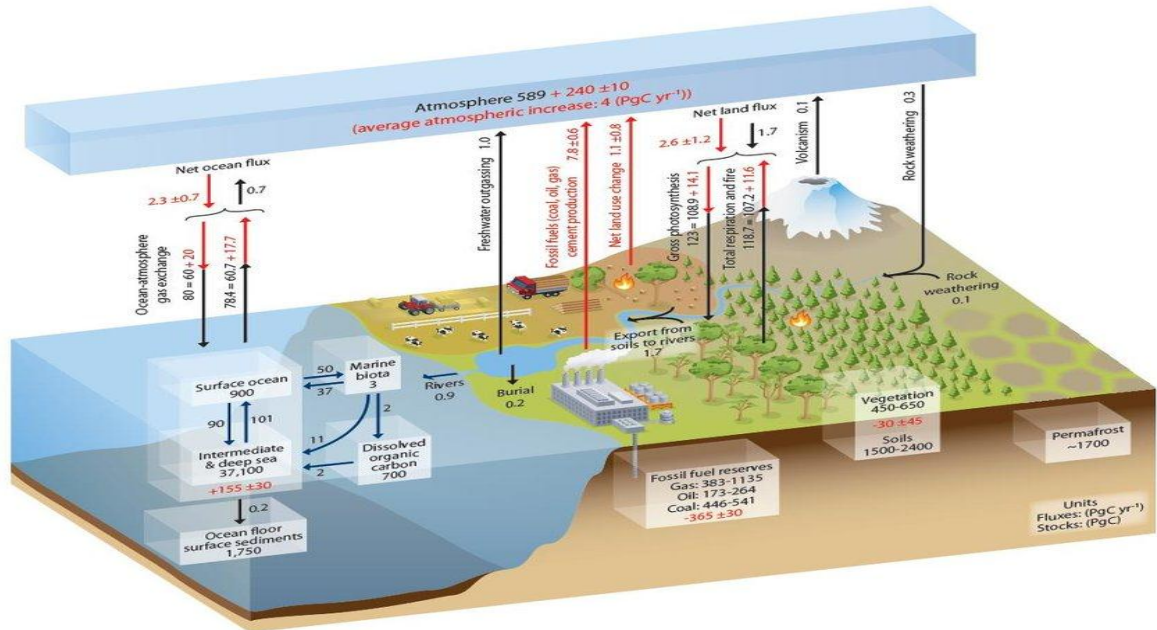


Figure 2.2: Simplified schematic overview of Global carbon cycle (IPCC,2013)

### 2.4.2 Methane Cycle

Methane ( $\text{CH}_4$ ) absorbs infrared radiation relatively stronger per molecule compared to  $\text{CO}_2$ , and it interacts with photochemistry. On the other hand, the methane turnover time is less than 10 years in the troposphere (Prather *et al.*, 2012). The sources of  $\text{CH}_4$  at the surface of the Earth can be thermogenic including natural emissions of fossil  $\text{CH}_4$  from geological sources (marine and terrestrial seepages, geothermal vents, and mud volcanoes) and emissions caused by leakages from fossil fuel extraction and use (natural gas, coal, and oil industry). There are also pyrogenic sources resulting from incomplete burning of fossil fuels and plant biomass (both natural and anthropogenic fires). The biogenic sources include natural biogenic emissions predominantly from wetlands, from termites, and very small emissions from the ocean. Anthropogenic biogenic emissions occur from rice paddy agriculture, ruminant livestock, landfills, man-made lakes and wetlands, and waste treatment. In general, biogenic  $\text{CH}_4$  is produced from organic matter under low oxygen conditions by fermentation processes of methanogenic microbes (Conrad,1996).

Atmospheric CH<sub>4</sub> is removed primarily by photochemistry, through atmospheric chemistry reactions with the OH radicals. Other smaller removal processes of atmospheric CH<sub>4</sub> take place in the stratosphere through reaction with chlorine and oxygen radicals, by oxidation in well-aerated soils, and possibly by reaction with chlorine in the marine boundary layer. The methane cycle is as shown below.

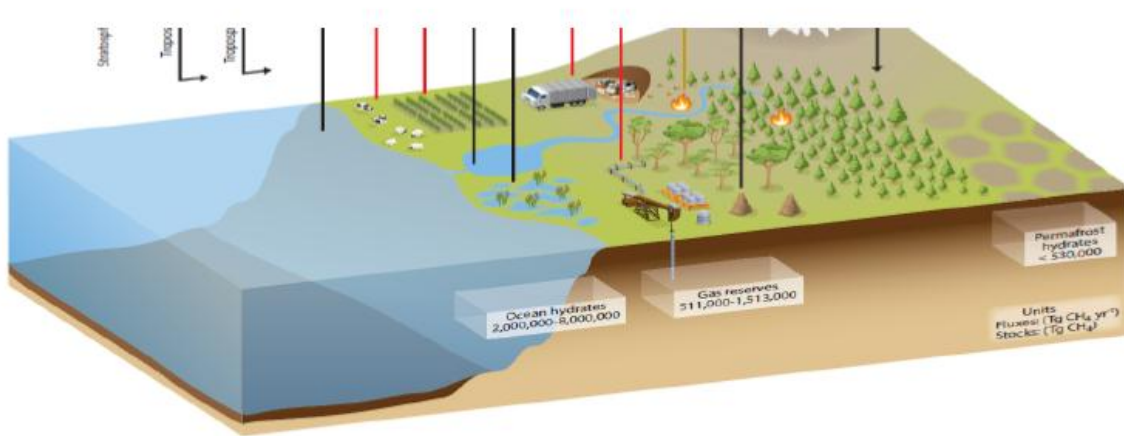


Figure 2.3: Simplified Schematic Overview of Global Methane Cycle (IPCC, 2013)

### 2.4.3 Nitrous Cycle

The biogeochemical cycles of nitrogen and carbon are tightly coupled with each other owing to the metabolic needs of organisms for these two elements. Changes in the availability of one element will influence not only biological productivity but also availability and requirements for the other element and in the longer term, the structure and functioning of ecosystems as well. Before the Industrial Era, the creation of reactive nitrogen Nr (all nitrogen species other than N<sub>2</sub>) from non-reactive atmospheric N<sub>2</sub> occurred primarily through two natural processes: lightning and biological nitrogen fixation (BNF). BNF is a set of reactions that convert N<sub>2</sub> to ammonia in a microbially mediated process. This input of Nr to the land and ocean biosphere was in balance

with the loss of Nr through denitrification, a process that returns  $N_2$  to the atmosphere. This equilibrium has been broken since the beginning of the Industrial Era. Nr is produced by human activities and delivered to ecosystems. During the last decades, the production of Nr by humans has been much greater than natural production. There are three main anthropogenic sources of Nr, the Haber-Bosch industrial process, used to make  $NH_3$  from  $N_2$ , for nitrogen fertilizers and as a feedstock for some industries, the cultivation of legumes and other crops, which increases BNF; and the combustion of fossil fuels, which converts atmospheric  $N_2$  and fossil fuel nitrogen into nitrogen oxides ( $NO_x$ ) emitted to the atmosphere and re-deposited at the surface. In addition, there is a small flux from the mobilization of sequestered Nr from nitrogen-rich sedimentary rocks (Morford *et al.*, 2011). The amount of anthropogenic Nr converted back to non-reactive  $N_2$  by denitrification is much smaller than the amount of Nr produced each year, that is, about 30 to 60% of the total Nr production, with a large uncertainty (Bouwman *et al.*, 2013). What is more certain is the amount of  $N_2O$  emitted to the atmosphere. Anthropogenic sources of  $N_2O$  are about the same size as natural terrestrial sources. In addition, emissions of Nr to the atmosphere, as  $NH_3$  and  $NO_x$ , are caused by agriculture and fossil fuel combustion. A portion of the emitted  $NH_3$  and  $NO_x$  is deposited over the continents, while the rest gets transported by winds and deposited over the oceans. This atmospheric deposition flux of Nr over the oceans is comparable to the flux going from soils to rivers and delivered to the coastal ocean (Suntharalingam *et al.*, 2012). The increase of Nr creation during the industrial era, the connections among its impacts, including on climate and the connections with carbon cycle are presented in the figure below.

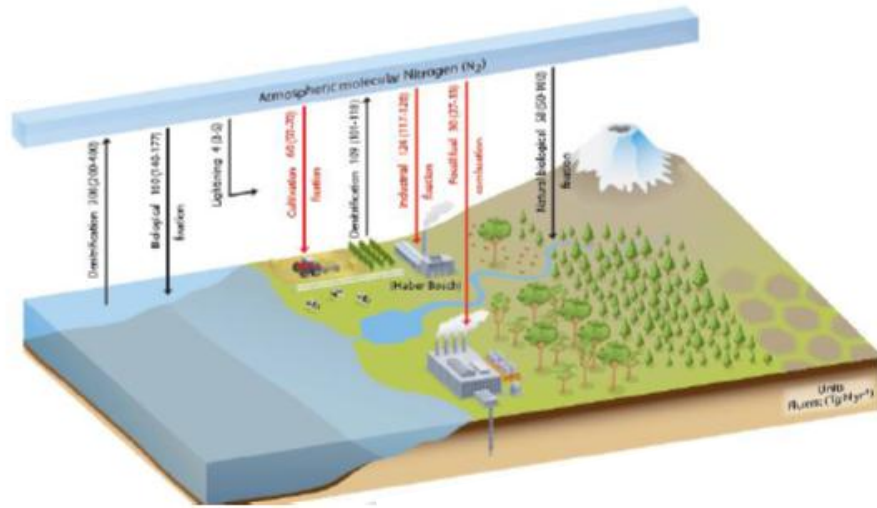


Figure 2.4 Simplified Schematic Overview of Global Nitrogen Cycle (IPCC, 2013)

## CHAPTER THREE

### MATERIALS AND METHODS

#### 3.1 Sampling areas

The areas sampled for this study is the Niger Delta but major oil exploration towns were picked as a reference point with their respective latitudes and longitudes are Eket ( Akwa Ibom) (07° 86'E, 04° 71'N), Oguta (Imo) (06° 81'E, 05° 87'N), Akpabuyo (Cross River) (06° 46'E, 07° 47'N), Port Harcourt (Rivers) (06° 90'E, 04° 76'N), Warri (Delta) (05° 18'E, 05° 63'N).

The choice of these locations was based on the factors explained in section 1.1. The temporal scale for all these data is monthly averages from 2013 to 2015.

#### 3.1.1 Data sets

The following datasets were acquired for this research as shown in table 3.1.

**Table 3.1: Data Instruments and uses**

Data	Use	Source
Atmospheric Infrared Sounder (AIRS)	To acquire the CO distribution	NASA
Ozone Monitoring Instrument (OMI AI)	Extract the absorbing aerosol index for each aerosol.	
NOAA HYSPLIT	Apportion the source, direction of transportation, and concentration of pollutants in the study areas	

### **3.2 Data Acquisition, Analysis, and Processing using GES-DISC (Goddard Earth Sciences Data and Information Services Center) Interactive Online Visualization and Analysis Infrastructure (GIOVANNI)**

The following dataset (AIRS CO, OMI/TOMS, NOAA HYSPLIT) were acquired, analyzed, and processed on a one-stop web-based platform known as GIOVANNI. It is a NASA data analysis and visualization system that provides a simple and intuitive way to visualize, analyze, and access vast amounts of Earth science remote sensing data, without having to download the data according to (Acker and Leptoukh, 2007). This online platform allows researchers to rapidly explore data, so that spatial-temporal variability, anomalous conditions, and patterns of interest can be directly analyzed online before the optional downloading of data. Giovanni was contributed to by many users' science research efforts and applications. GIOVANNI is a useful tool for data exploration, acquisition, analysis, and research uses in remote sensing. The advantage of using GIOVANNI is that it allows users to explore various atmospheric remote sensing data without necessarily learning about the data formats and battling with memory space. The following data sources were employed in the execution of this project, we dwelt mostly on satellite data, which has the advantage of maintaining a continuous uninterrupted observation, covering a large spatial-temporal area.

### **3.3 Ozone Monitoring Instrument (OMI)**

Ozone Monitoring Instrument (OMI) flown on the EOS Aura spacecraft (launched July 2004), is a data continuation Total Ozone Mapping Spectrometer (TOMS) whose data was acclaimed to be the longest continuous satellite-based data acquisition platform available for use in monitoring global and regional trends for the past 37 years. Both platforms provide measurements of tropospheric aerosols, SO<sub>2</sub>, ultraviolet irradiance, erythemal UV exposure, and effective

reflectivity from the Earth's surface and clouds. Four TOMS instruments have been successfully flown in orbit aboard the Nimbus-7 (Nov. 1978 - May 1993), Meteor-3 (Aug. 1991 - Dec. 1994), Earth Probe (July 1996 - current), and ADEOS (Sep. 1996 - June 1997) satellites. These include level 3 gridded data ( $1.0^\circ \times 1.25^\circ$ ) as well as level 2 instrument resolution data (between  $50 \times 50$  km and  $26 \times 26$  km pixel at nadir). The key objectives of the instrument according to (Ahmad *et al.*, 2003) include monitoring of aerosols and smokes from biomass burning,  $\text{SO}_2$ , and key tropospheric pollutants and surface UV radiation that are a threat to human health. Because of better measurement accuracy and better spatial resolution ( $13 \times 24$  km), TOMS and OMI provide better estimates of atmospheric pollutants and their transport through the Earth's atmosphere (Liu *et al.*, 2012). The parameters of interest acquired by this sensor are  $\text{NO}_2$  and  $\text{SO}_2$ . AI is a qualitative indicator of the presence of absorbing aerosols and many scientists have used it in a variety of applications with encouraging results. Like most of the satellite aerosol retrievals, the TOMS and OMI  $\text{NO}_2$  and  $\text{SO}_2$  products have been validated by comparing them with ground measurements at a global scale, (Lu *et al.* 2015).

### **3.4 Atmospheric Infrared Sounder (AIRS)**

The Atmospheric Infrared Sounder (AIRS) instrument is flying on board of Aqua satellite. It was deployed on 4 May 2002. It has a cross-track scanning grating spectrometer that measures IR radiation at 2378 channels between 3.7 and  $16 \mu\text{m}$  with a 13.5 km nadir field of view (Aumann *et al.*, 2003). The AIRS suite constitutes an innovative atmospheric sounding system of infrared, microwave, and visible sensors. This product is the most accurate and stable set of hyperspectral infrared radiance spectra measurements made in space to date, and it meets the criteria identified by the National Research Council for climate data records. The geophysical products provide daily global temperature profiles at an accuracy of 1 K per 1 km thick layer in the troposphere

and moisture profiles at an accuracy of 20% per 2 km thick layer in the lower troposphere (20% - 60% in the upper troposphere). With the Version 5 release, the Level-2 and Level-3 products also include the burden and profiles of the minor gases such as O<sub>3</sub> (Level-2 only), CO, and CH<sub>4</sub>. It is considered a robust retrieval because of its strong spectral signature and weak water vapor interference with an estimated accuracy of about 15%.

### **3.5 NOAA Hybrid Single-Particle Integrated Trajectory(HYSPLIT)**

The NOAA HYSPLIT model was used to apportion the source, direction of, transportation, and concentration of pollutants in the study area. A model is a tool that helps explain how, when, and where potentially harmful materials are atmospherically transported, dispersed, and deposited. Having this understanding is essential for responding appropriately and preventing disaster. The HYSPLIT model is a complete system for manipulating simple air parcel trajectories to complex dispersion and deposition simulations. The model is a hybrid between the Lagrangian approach, which uses a moving frame of reference for the advection and diffusion calculations as the air parcels move from their initial location, and the Eulerian approach, which uses a fixed three-dimensional grid as a frame of reference to compute the pollutant air concentrations (Draxler *et al.*, 1998). Its applications include:

Tracking and forecasting the release of pollutant material.

Air-parcel trajectories.

Volcanic ash, and smoke from wildfires.

It makes use of gridded meteorological data to drive the trajectories and concentrations either forwards or backward in time at regular time intervals. In this study, we made use of the forward trajectory which gave us the direction, concentration, and where pollutants are deposited from and specified location.

### 3.6 Location and Physiography of the Study Area

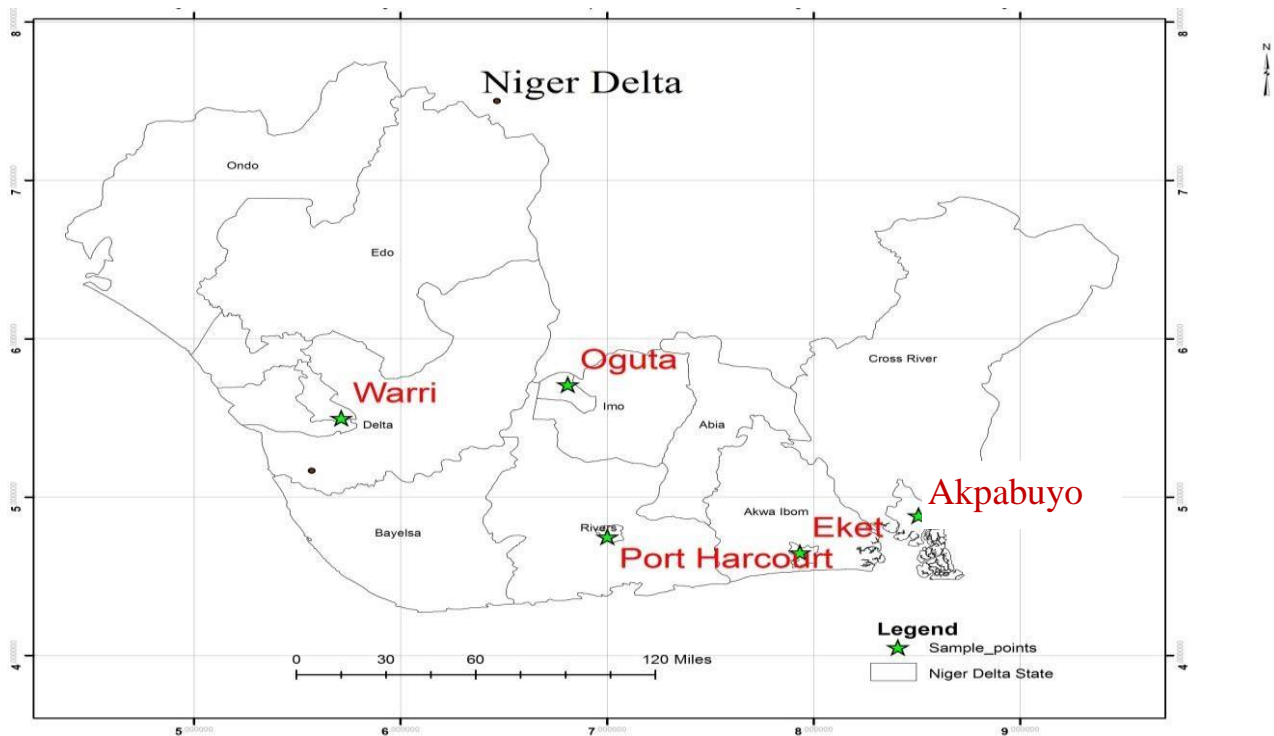
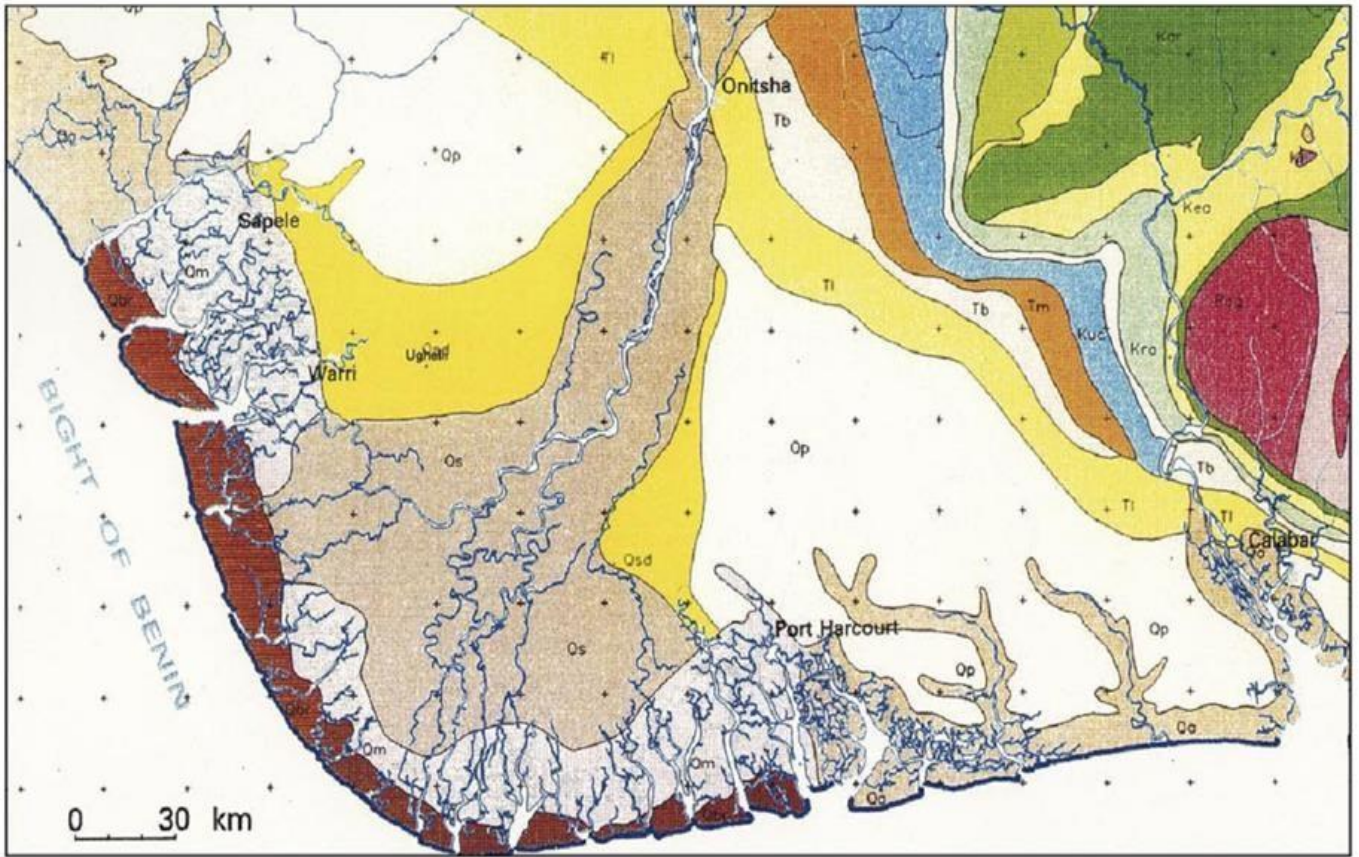


Figure 3.1: Map showing locations of the study area

### 3.7 Geology of the Study Area

The Niger Delta covers an area of approximately 75,000km<sup>2</sup> and consists of a regressive sequence whose maximum thickness is about 12km in the central part (Short & Stauble, 1967). It is one of the most prominent basins in West Africa and the largest delta in Africa (Reijers, 2011). It ranks among the world's most prolific petroleum-producing tertiary deltas that together account for about 5% of the world's oil and gas reserves and about 2.5% of the present-day basin of the earth. The figure below shows the geological map of the Niger delta.



QUATERNARY		CRETACEOUS	
meander belt, back swamps	Qa alluvium	Falsebedded sst. and U. coal measures	Kuc Falsebedded sst., coal and shale
fresh water swamps	Qs sands, gravels and clays	lower coal measures	Klc coal, sandstone and shale
mangrove swamps	Qm sands, clays and mangrove swamps	Nkporo shale group	Kro shale and mudstone
abandoned beach ridges	Qbr sands and pebbles	Cretaceous intrusion	Ki basic and intermediate intrusions
Sombreiro deltaic plain	Qsd sands, clay and mangrove swamps	Awgu-Ndeabah shale group	Kwn shale and limestone
coastal plains sands	Qp sands and clays	Eze Aku shale group	Kea black shale and siltstone
		Odukpani formation	Kc flaggy shale and calcareous sst.
		Asu river group	Kar shale and limestone
TERTIARY		PRE-CAMBRIAN TO UPPER CAMBRIAN	
lignite formation	Ti clays, sst., lignite and shales	basement complex	Pcg older granite
Bende Ameki group	Tb clays, clayey sands and shale		
Imo clay-shale group	Tm clays and shales with lst.		

Figure 3.2 Geological Map of Niger Delta and its surroundings (Reijers, 2011)

The study area for this project is in five (5) locations of the Niger Delta. The region (Niger Delta) is situated in the southern part of Nigeria and bordered to the south by the Atlantic Ocean and the East by Cameroon, it occupies a surface area of about 112,110 square kilometres. It represents about 12% of Nigeria's total surface area and it is estimated that by the beginning of 2006 its population will be over 28 million inhabitants. (NDRDMP, 2000).

### **3.7.1 Vegetation**

The Niger Delta Region is a rich and diverse mosaic of ecological types. Five distinct ecological zones are ranging from the barrier island forest and coastal vegetation areas through to Montane habitats.

### **3.7.2 Relief**

The pattern of settlement in the Niger Delta Region is largely determined by the availability of dry land and the nature of the terrain. Low relief and poor ground drainage are the primary factors responsible for the low number of large settlements in the region. The larger settlements are found in the interior parts of the Delta, which has better drainage conditions and accessibility. In the mangrove swamp zone, the main settlements such as Port Harcourt, Sapele, Ughelli, and Warri, have developed on islands of dry land that intersperse the zone with settlements being located at the head of the navigable limits of the coastal rivers or estuaries. In total, there are 13,329 settlements in the Niger Delta Region. The average population of 13,231 of these (99% of the total) falls below 20,000 people.

Settlements of fewer than 5,000 inhabitants constitute nearly 94% of the total number of settlements and only 98 settlements, that is less than 1% of the settlements, can be truly regarded as urban centres according to their population sizes. The main towns in this category include Port Harcourt, Warri, Asaba, Benin, Akure, Calabar, Uyo, Umuahia, Aba, Owerri, and Yenagoa. The

predominant settlement type in the Niger Delta is small and scattered hamlets. The vast majority of settlements comprise largely rural communities in dispersed village settlements. The typical community consists of compounds, which are closely spaced groups of small buildings housing 50 to 500 people, most of whom are farmers or fisherfolk. There are also larger settlements, which are usually separated from other clusters of rural residences by their outer, rotational farmlands, oil palm or rubber plantation, bush, or stretches of secondary forest. These towns are usually located along roads, which radiate from a 'core' where churches, schools, markets places, and other functions are situated. Most rural settlements lack essential amenities, such as medical facilities, efficient marketing services, adequate shopping facilities, good water, power supply, and good transportation systems.

### **3.7.3 Climate**

The climate of the Niger Delta Region varies from the hot equatorial forest type in the southern lowlands to the humid tropical in the northern highlands and the cool montane type in the Obudu plateau area. The wet season is relatively long, lasting between seven and eight months of the year, from March to October. In the northern and north-western parts of the Niger Delta Region, the rains may be delayed by as much as four weeks, thereby extending the dry season which, in recent times, tends to last some four to five months. There is usually a short break around August, otherwise termed the "August break". The dry season begins in late November and extends to February or early March, a period of approximately three months. During the dry season, the northeast trade wind blowing over the Sahara Desert extends its dehydrating influence progressively towards the equator, reaching the southern coast of Nigeria in late December or early January. The period is known as the "Harmattan", which is more noticeable in some years than others. Mean annual rainfall ranges from over 4,000mm in the coastal towns of Bonny and Brass in Rivers and the Bayelsa States respectively, and decreases inland to 3,000mm

in the mid-delta around Ahoada, Yenagoa and Warri in Rivers, Bayelsa and the Delta States, respectively; and slightly less than 2,400mm in the northern parts of the region in Imo and the Abia States. In the northwestern portions including Edo and Ondo States, annual rainfall ranges from 1,500 - 2,000mm.

Temperatures are generally high in the region and fairly constant throughout the year. Average monthly maximum and minimum temperatures vary from 28<sup>0</sup>c to 33<sup>0</sup>c and 21<sup>0</sup>c to 23<sup>0</sup>c, respectively, increasing northward and westward. The warmest months are February, March, and early April in most parts of the Niger Delta Region. The coolest months are June through to September during the peak of the wet seasons.

### 3.8 Model for Data Integration

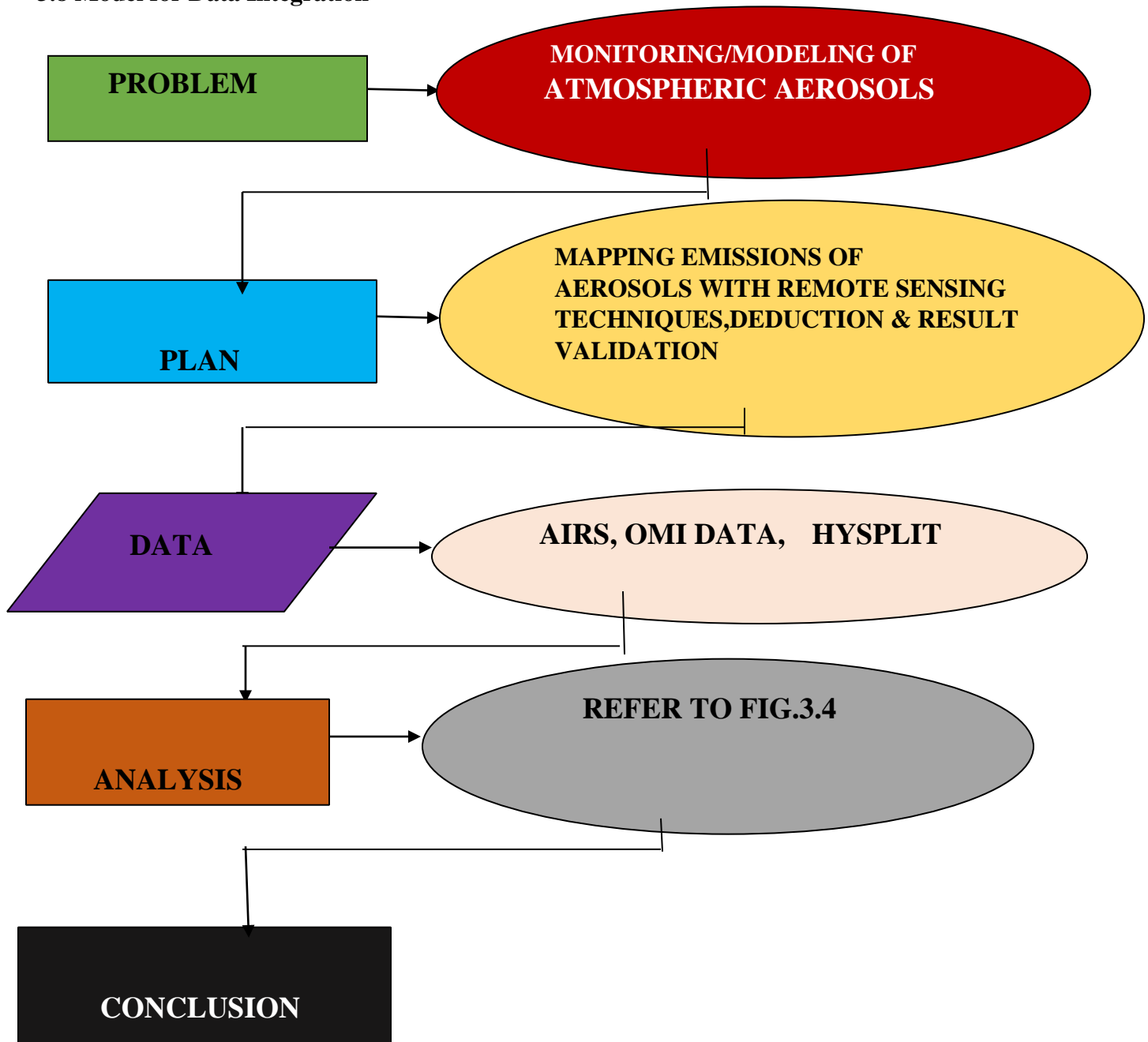


Figure 3.3: Data Integration

### 3.9 WORKFLOW

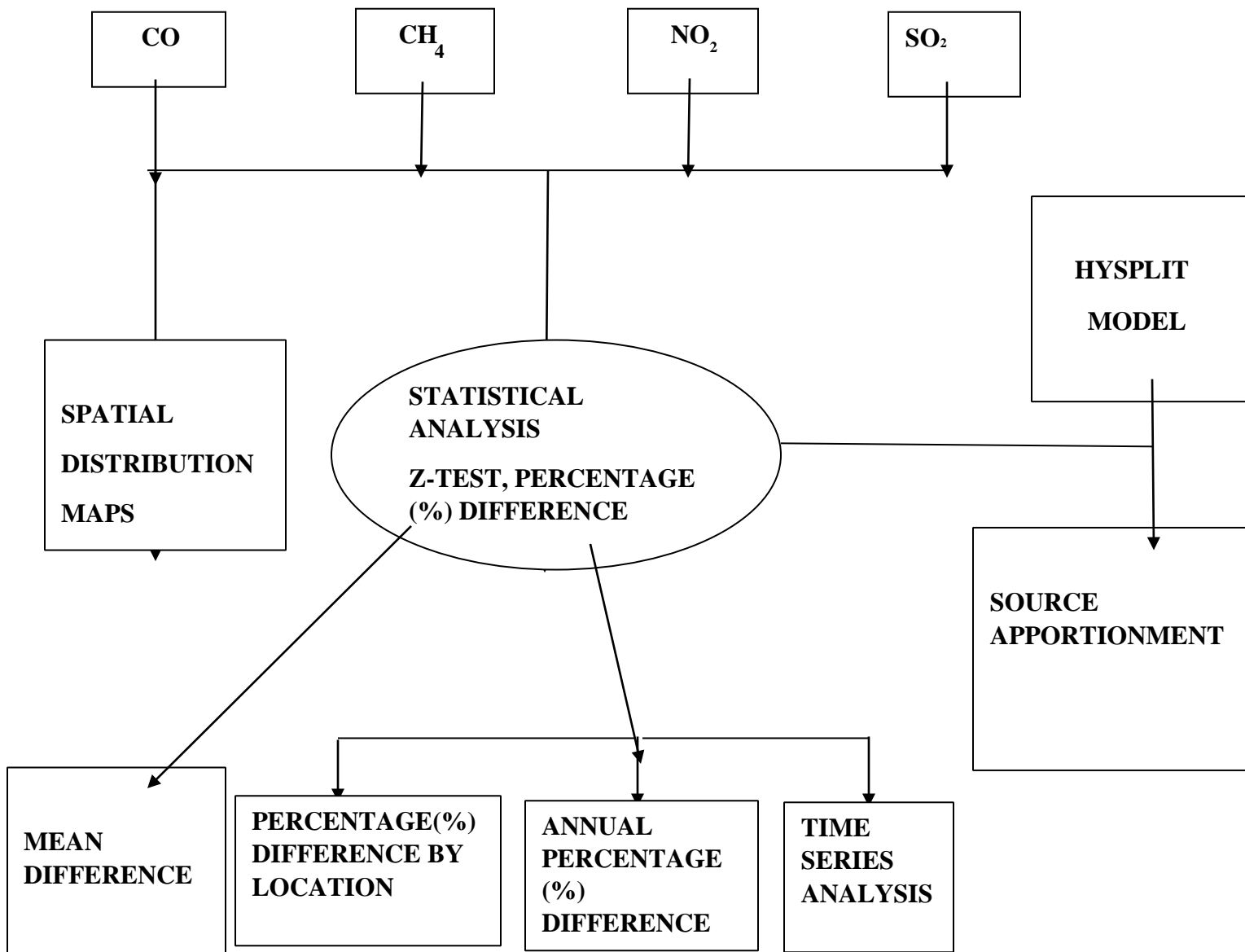


Figure 3.4: Workflow

## **CHAPTER FOUR**

### **RESULTS AND DISCUSSION**

#### **4.1 Seasonality of Atmospheric Species: Times Series Plot**

##### **(A) Methane (CH<sub>4</sub>)**

The time series plots for the areas under investigation are presented in Figure 4.1. The result shows that December (dry season) is the peak of CH<sub>4</sub> emission in all the study locations due to dry deposition, with Warri having the highest value ( $3.86 \times 10^{19}$  mol/cm<sup>2</sup>), Port Harcourt ( $3.82 \times 10^{19}$  mol/cm<sup>2</sup>) Eket ( $3.80 \times 10^{19}$  mol/cm<sup>2</sup>), Oguta ( $3.79 \times 10^{19}$  mol/cm<sup>2</sup>), while the least values were recorded in Akpabuyo ( $3.75 \times 10^{19}$  mol/cm<sup>2</sup>), during the rainy season in June due to wet deposition

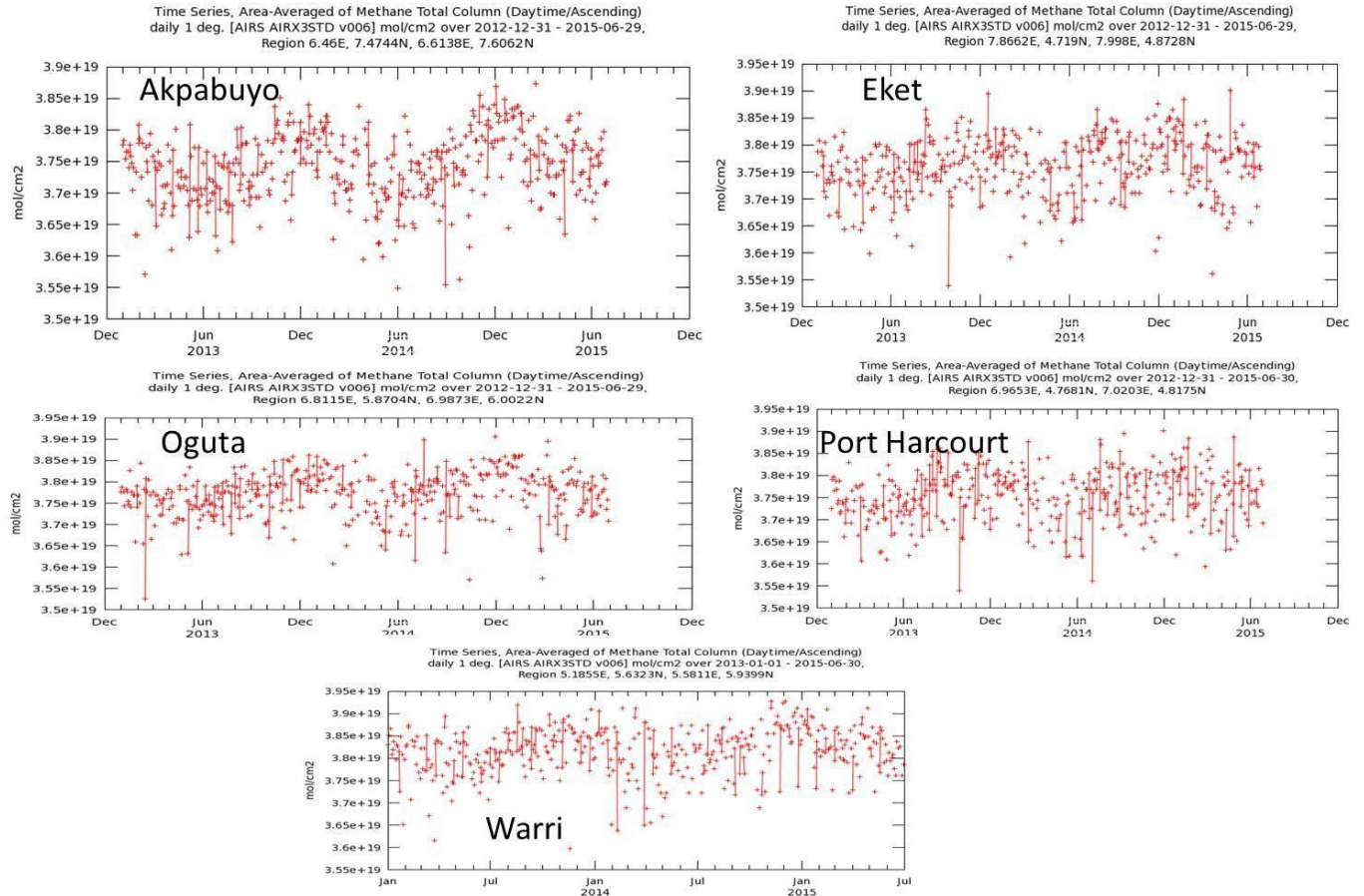


Figure 4.1: Time series of the plot of CH<sub>4</sub> emission from January 2013-June 2015.

**(B) Sulphur dioxide (SO<sub>2</sub>)**

The time series plotted for SO<sub>2</sub> on the OMI model, shows that SO<sub>2</sub> is at its peak in the dry season between January and March each year with PHC having values between (0 - 0.5 mmol/cm<sup>2</sup>), Warri (0.4 mol/cm<sup>2</sup>), Akpabuyo (0.4 mol/cm<sup>2</sup>), Oguta (0.3- 0.5 mmol/cm<sup>2</sup>), and Eket with the least value below -0.3 mol/cm<sup>2</sup>.

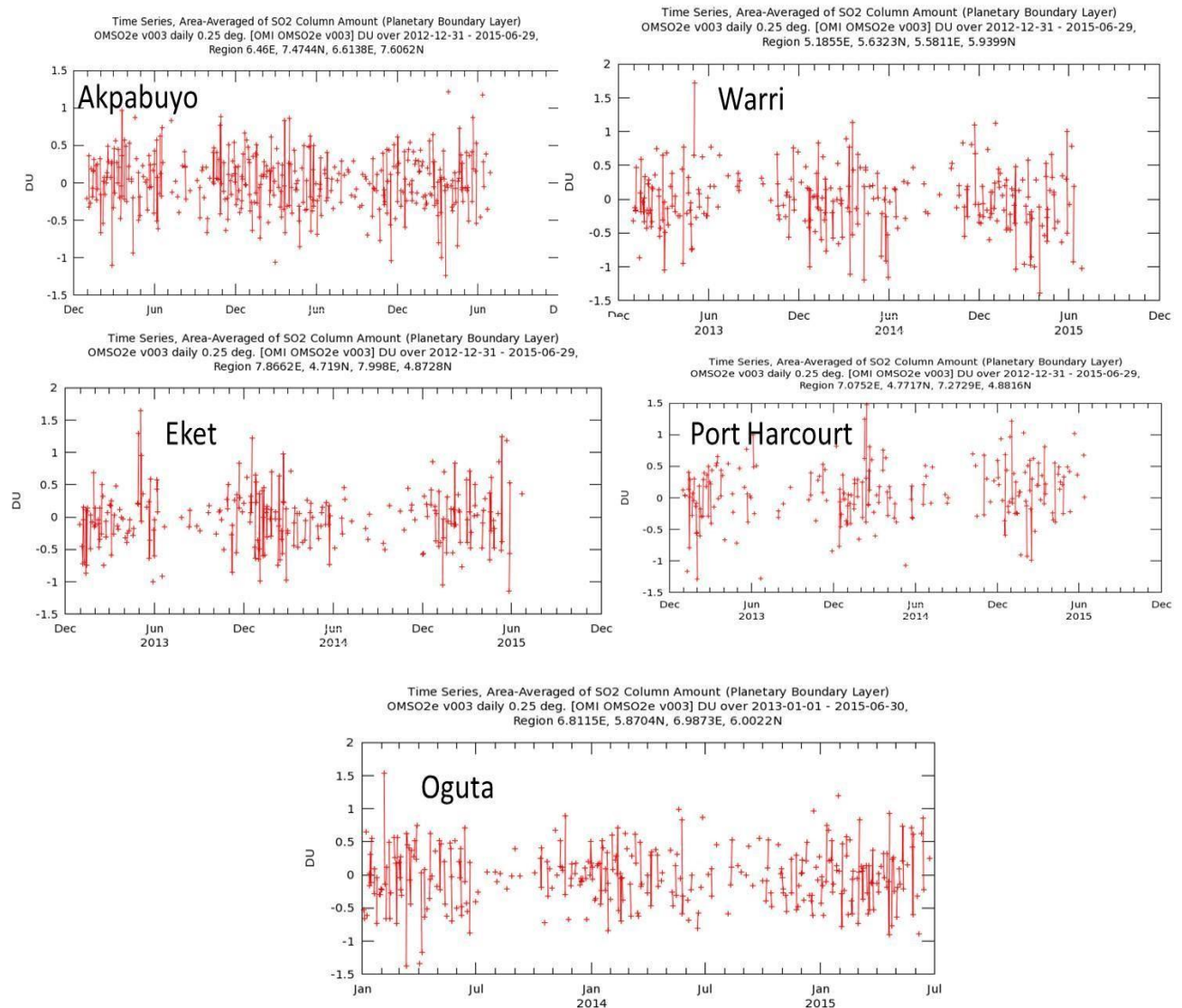


Figure 4.2: Time series of the plot of SO<sub>2</sub> emission from January 2013-June 2015

**(C) Carbon Monoxide (CO)**

The CO emission time series on the AIRS model, shows a distinct curve pattern in all the locations, where emission increases from January-April due to sedimentation, with Akpabuyo having the highest value ( $3.3 \times 10^{18} \text{ mol/cm}^2$ ), Oguta ( $3.0 \times 10^{18} \text{ mol/cm}^2$ ), Warri ( $2.95 \times 10^{18} \text{ mol/cm}^2$ ), Eket ( $2.9 \times 10^{18} \text{ mol/cm}^2$ ), PHC ( $2.8 \times 10^{18} \text{ mol/cm}^2$ ). This analysis also shows that

CO emission maintains double maxima in Nigeria at the peak of the dry season and August break.

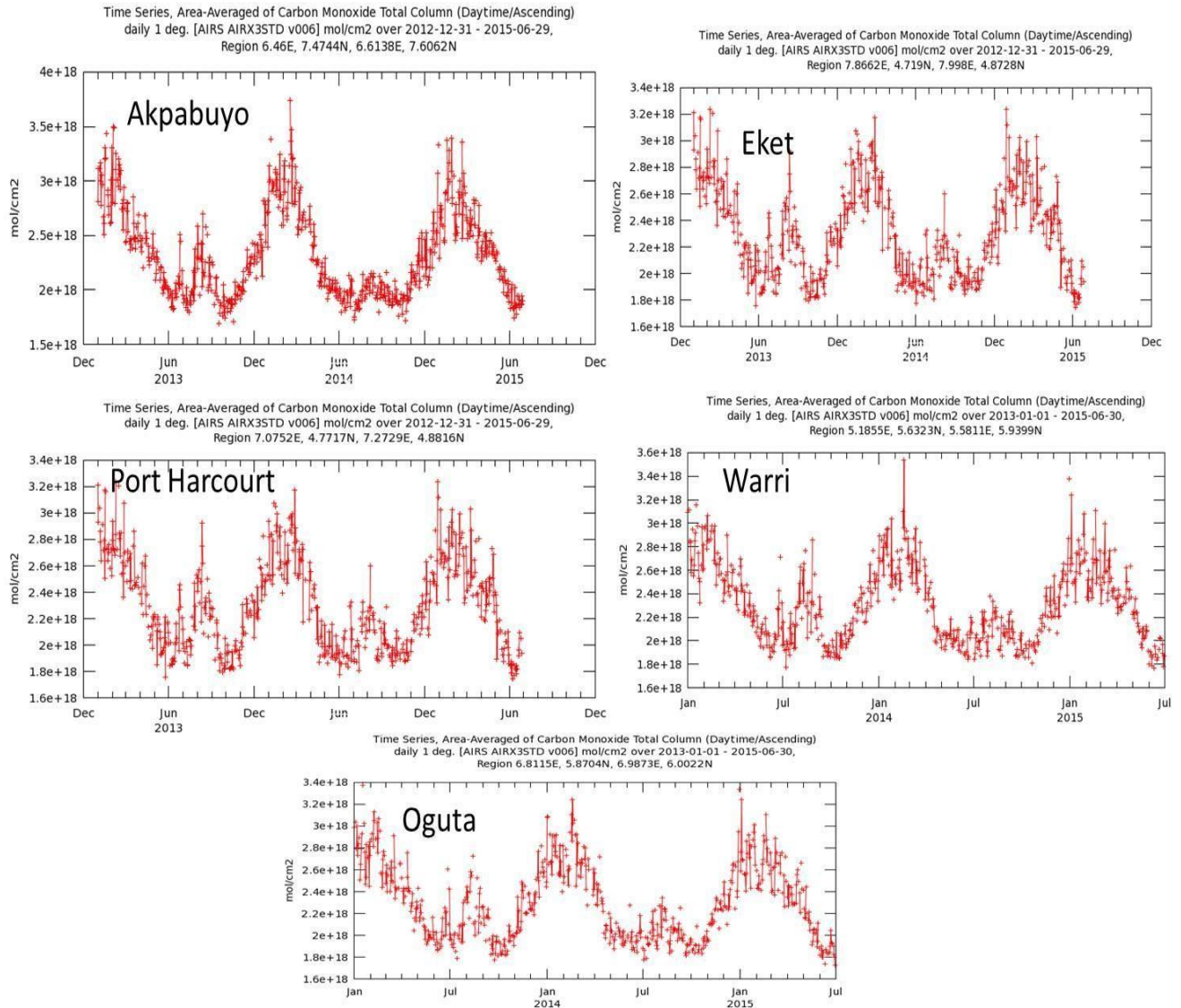


Figure 4.3: Time series of the plot of CO emission from January 2013-June 2015

**(D) Nitrogen (iv) Oxide (NO<sub>2</sub>)**

The curves in figure 4.4, show that NO<sub>2</sub> emissions in all the study locations maintain a January peak and a rainy season trough between September and August. plotted on the OMI Model with the highest recorded in

Oguta( $5.3 \times 10^{15}$   $1/\text{cm}^2$ ), PHC( $5.2 \times 10^{15}$   $1/\text{cm}^2$ ), Warri ( $4.9 \times 10^{15}$   $1/\text{cm}^2$ ), Akpabuyo( $4.7 \times 10^{15}$   $1/\text{cm}^2$ ) and Eket with the least value of ( $4.6 \times 10^{15}$   $1/\text{cm}^2$ ).

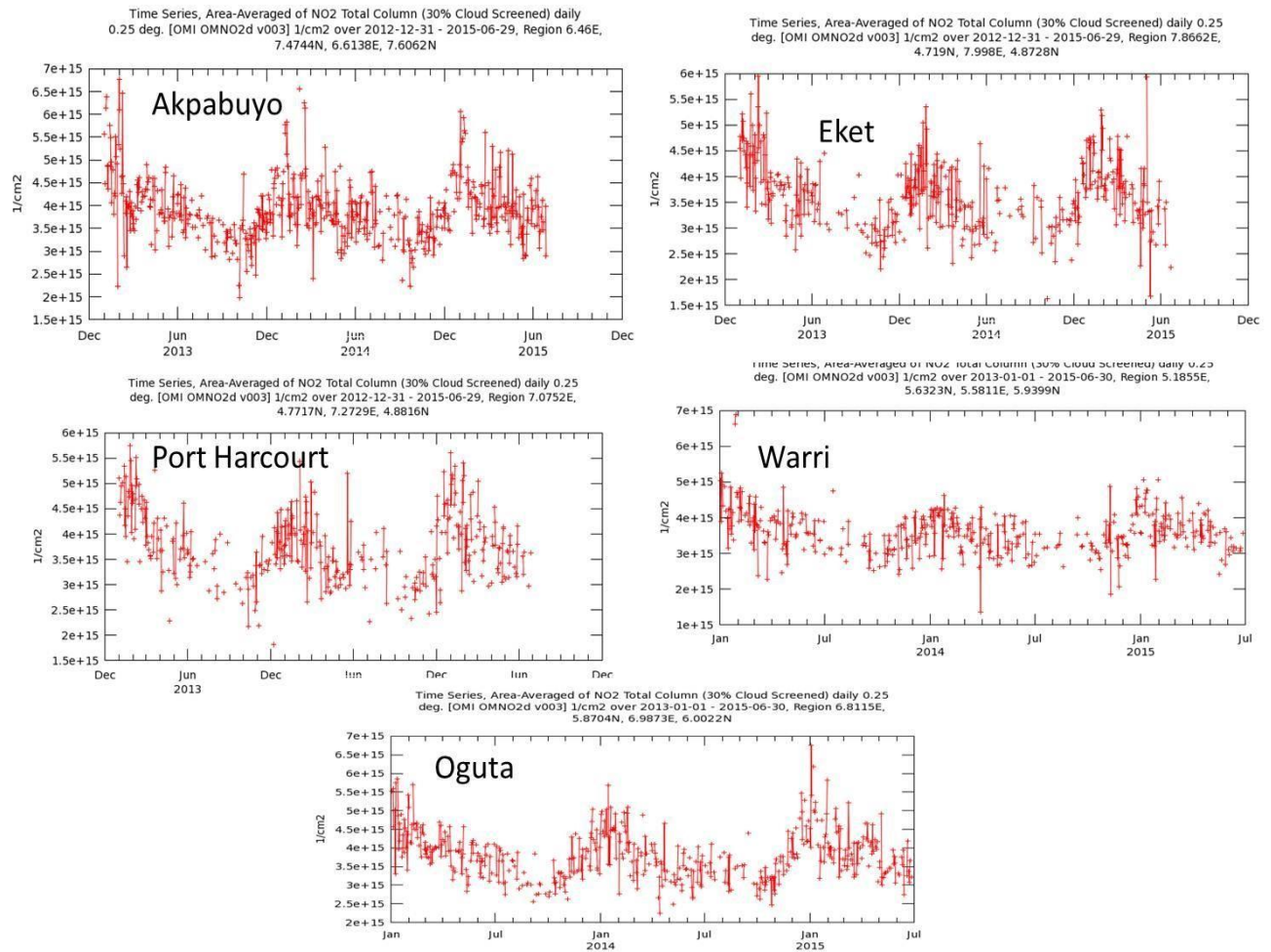


Figure 4.4: Time series of the plot of NO<sub>2</sub> emission from January 2013-June 2015.

The general deduction from the various time series shows that:

1. The gas emission follows a seasonal pattern. This implies that a variety of sources such as crude oil drilling, gas flaring, vehicular emissions, etc contributes to their emissions.

#### **4.1.1 HYSPLIT MODELS FOR EACH LOCATION**

The results showed a forward trajectory which gave the direction, concentration, and where pollutants are deposited from and specified location at an altitude of 0, 50, 100m above ground level (AGL).

**(A) OGUTA**

The figure below shows that in Oguta the maximum travel distance is 10km.

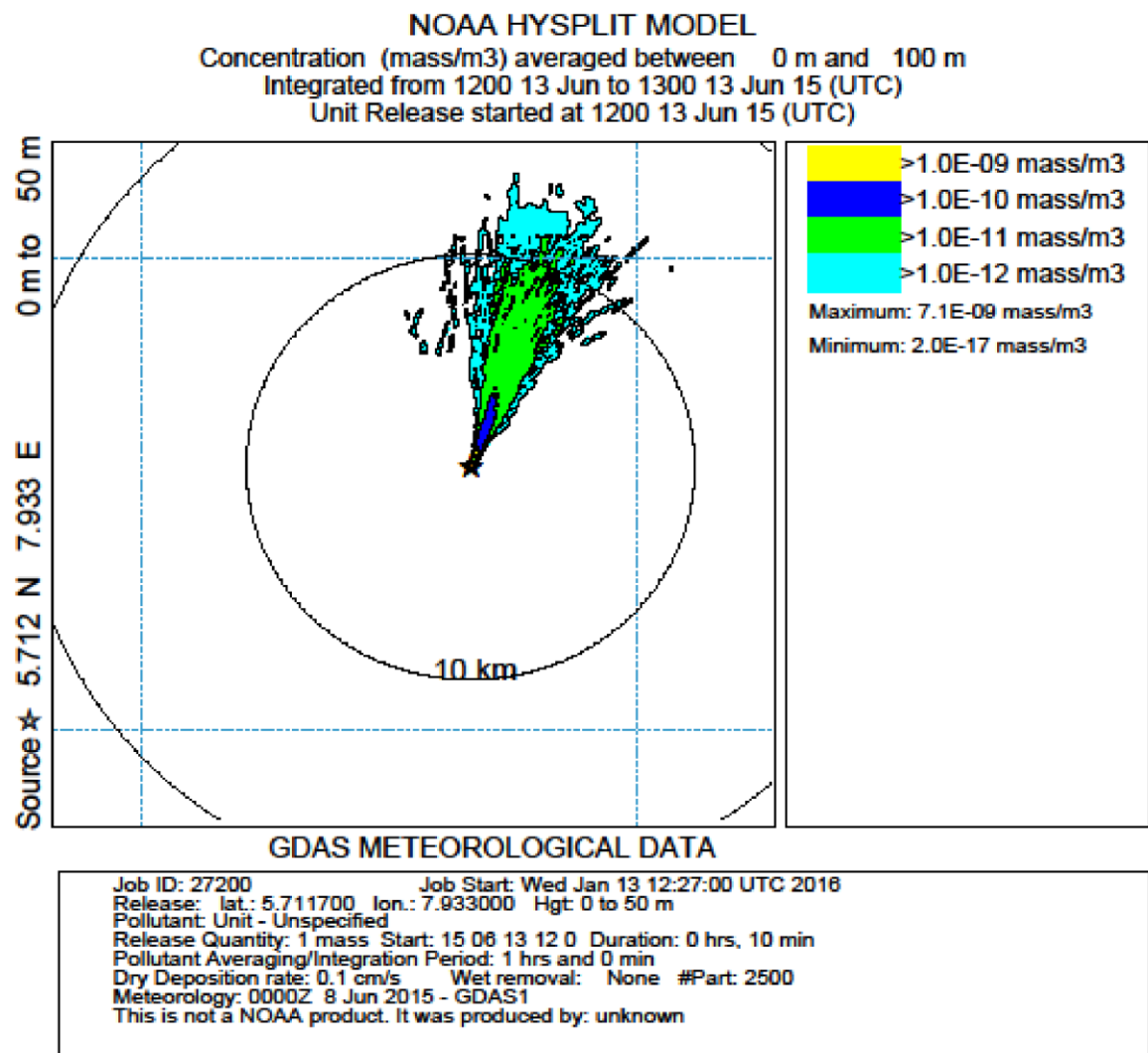


Figure 4.5: HYSPLIT model showing the concentration of pollutants in Oguta

**(B) Port Harcourt**

The figure below shows the travel distance for Port Harcourt at a radius of influence of 40km

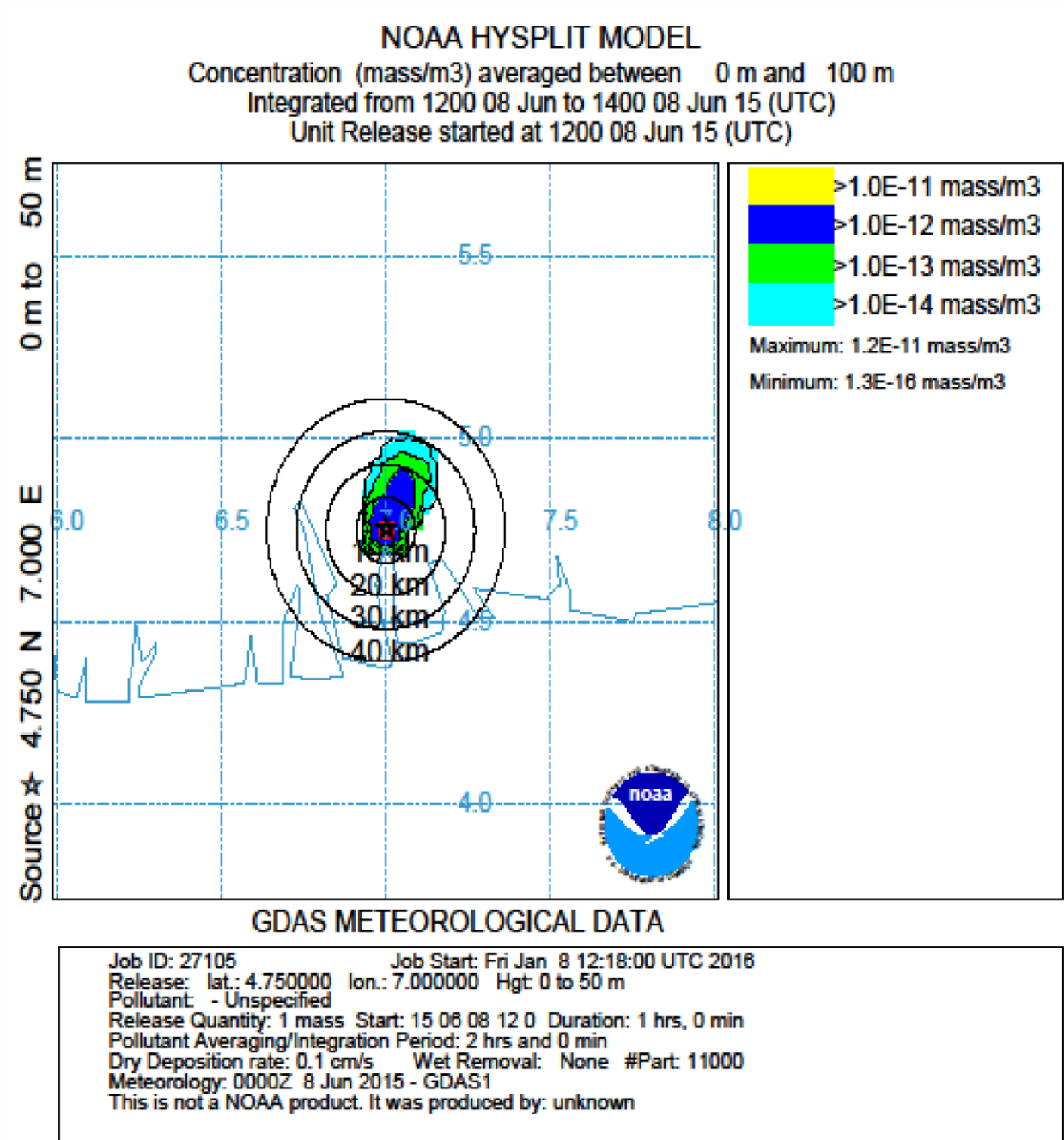


Figure 4.6: HYSPLIT model showing the concentration of pollutants in PHC

**(C)Warri**

The figure below shows that Warri has a radius of influence of 40km.

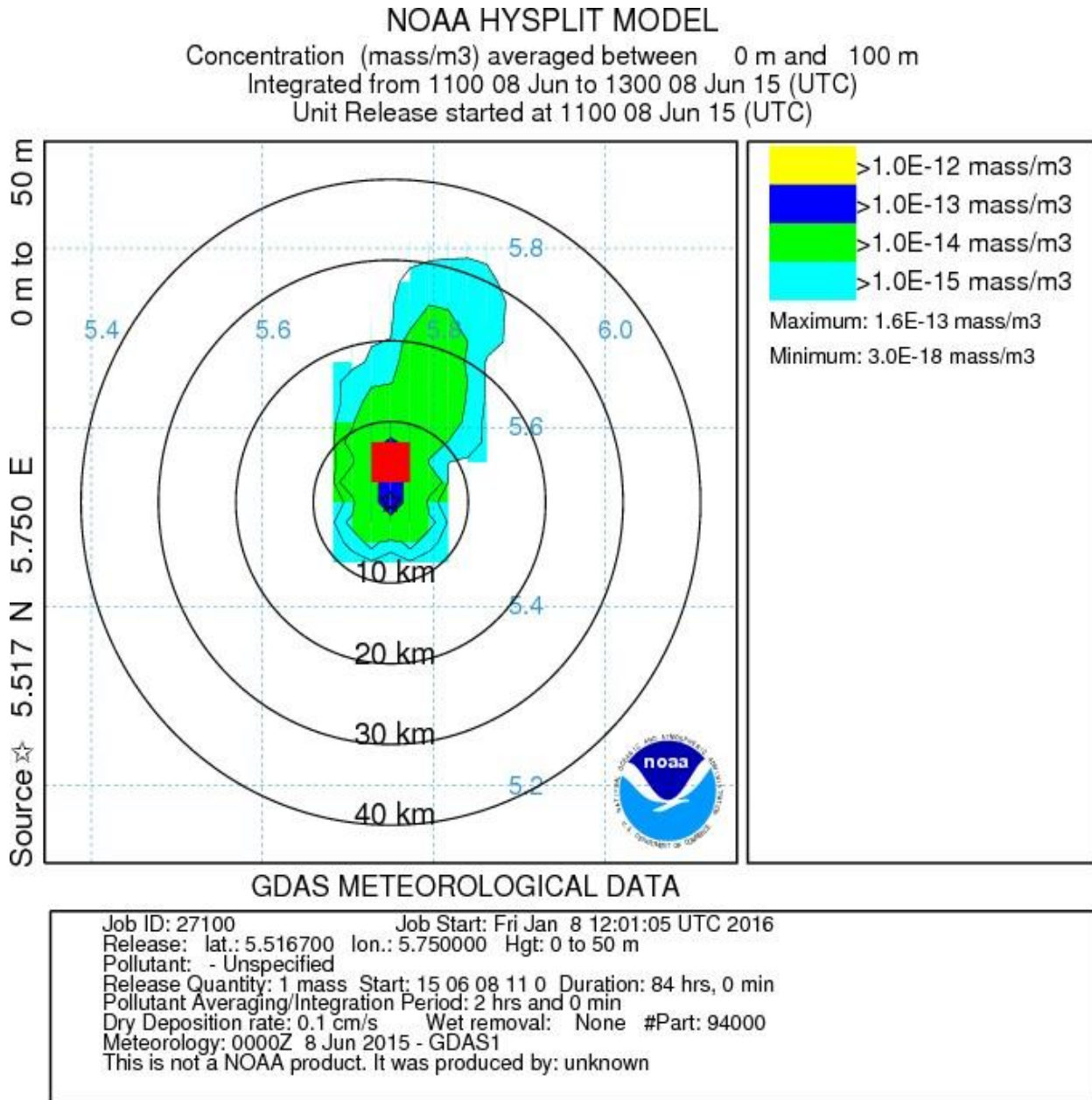


Figure 4.7: HYSPLIT model showing the concentration of pollutants in Warri

(D) Eket

For Eket, the figure below shows that the maximum travel distance is 40km.

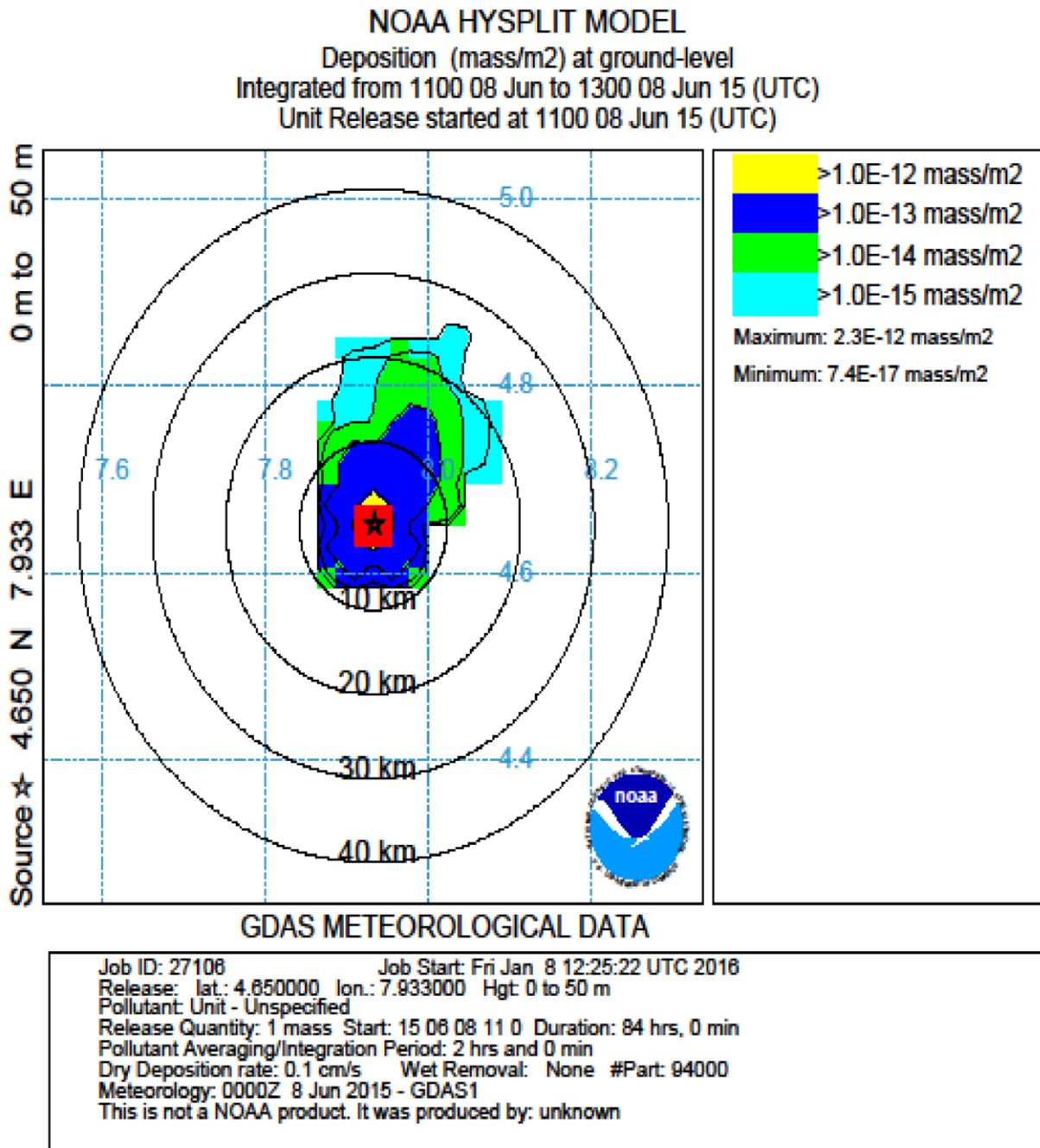


Figure 4.8: HYSPLIT model of species deposition from Eket

**(E) Akpabuyo**

The radius of influence for Akpabuyo is 10km as shown in the figure below.

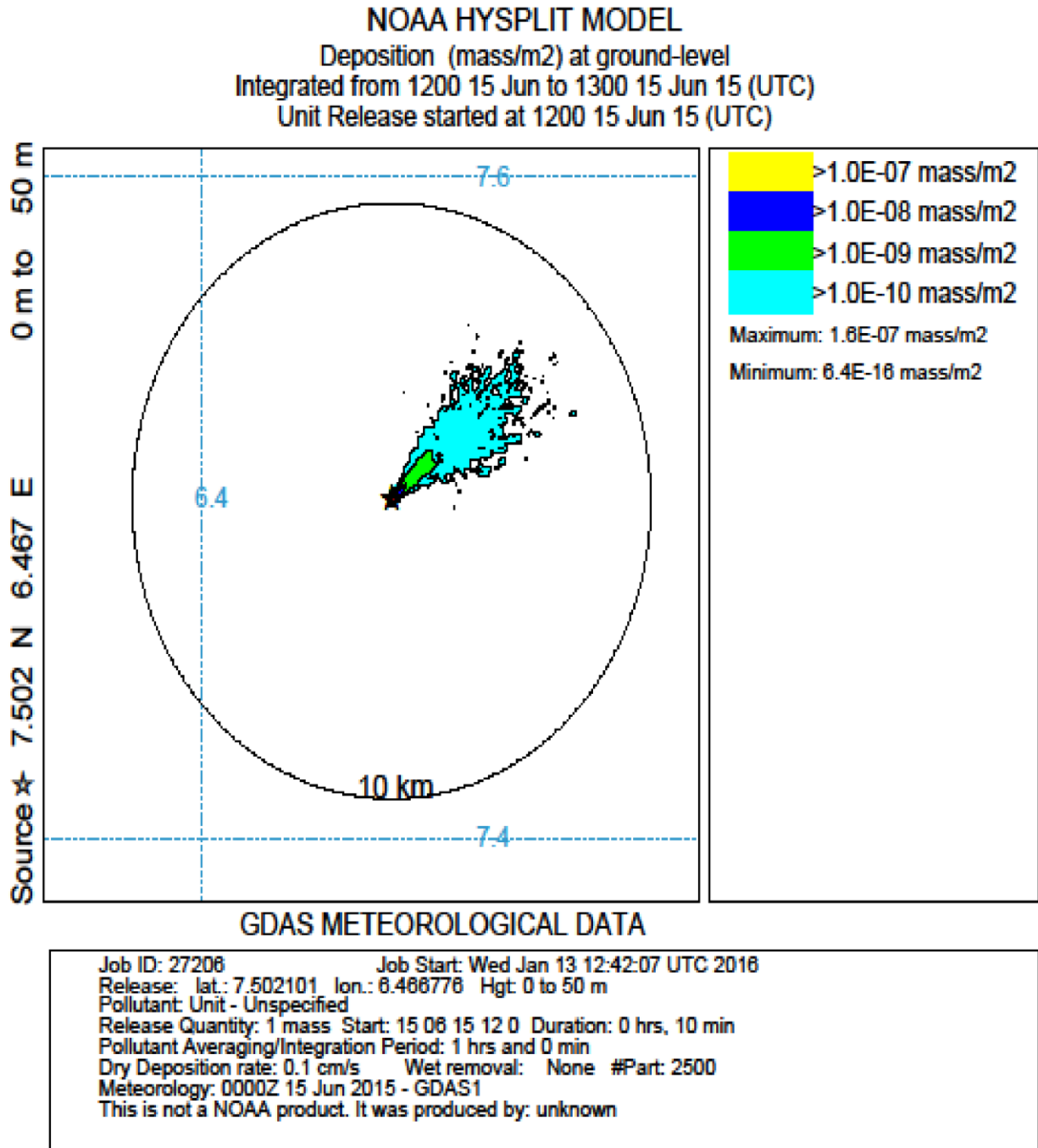


Figure 4.9: HYSPLIT model of species deposition from Akpabuyo.

**Table 4.1: Distance of deposition of particle**

<b>Location</b>	<b>Radius of influence (Km).</b>	<b>Maximum travel of distance (Km)</b>
<b>Port Harcourt</b>	40	40
<b>Oguta</b>	10	10
<b>Eket</b>	40	40
<b>Warri</b>	40	40
<b>Akpabuyo</b>	10	10

From figures above, the HYSPLIT model shows that particles are dispersed towards North of Port Harcourt where Oguta is located. Hence, Oguta receives an enormous volume of gases from Port Harcourt due to the high wind speed regime and also the topography. A look at the HYSPLIT model for Oguta showed that the species does not travel a long distance before being deposited (deposited within 10km),(Table 4.1). This implies that pollutants are deposited around Oguta and environs from where most of them are generated.

#### 4.1.2 SPATIAL DISTRIBUTION MAPS:

Spatial attributes of the atmospheric aerosols were determined, which revealed areas with elevated values of the pollutants in a choropleth map layer.

(i) **Methane Emissions:** The result indicated elevated values of CH<sub>4</sub> observed in Akpabuyo followed by Port Harcourt as shown below.

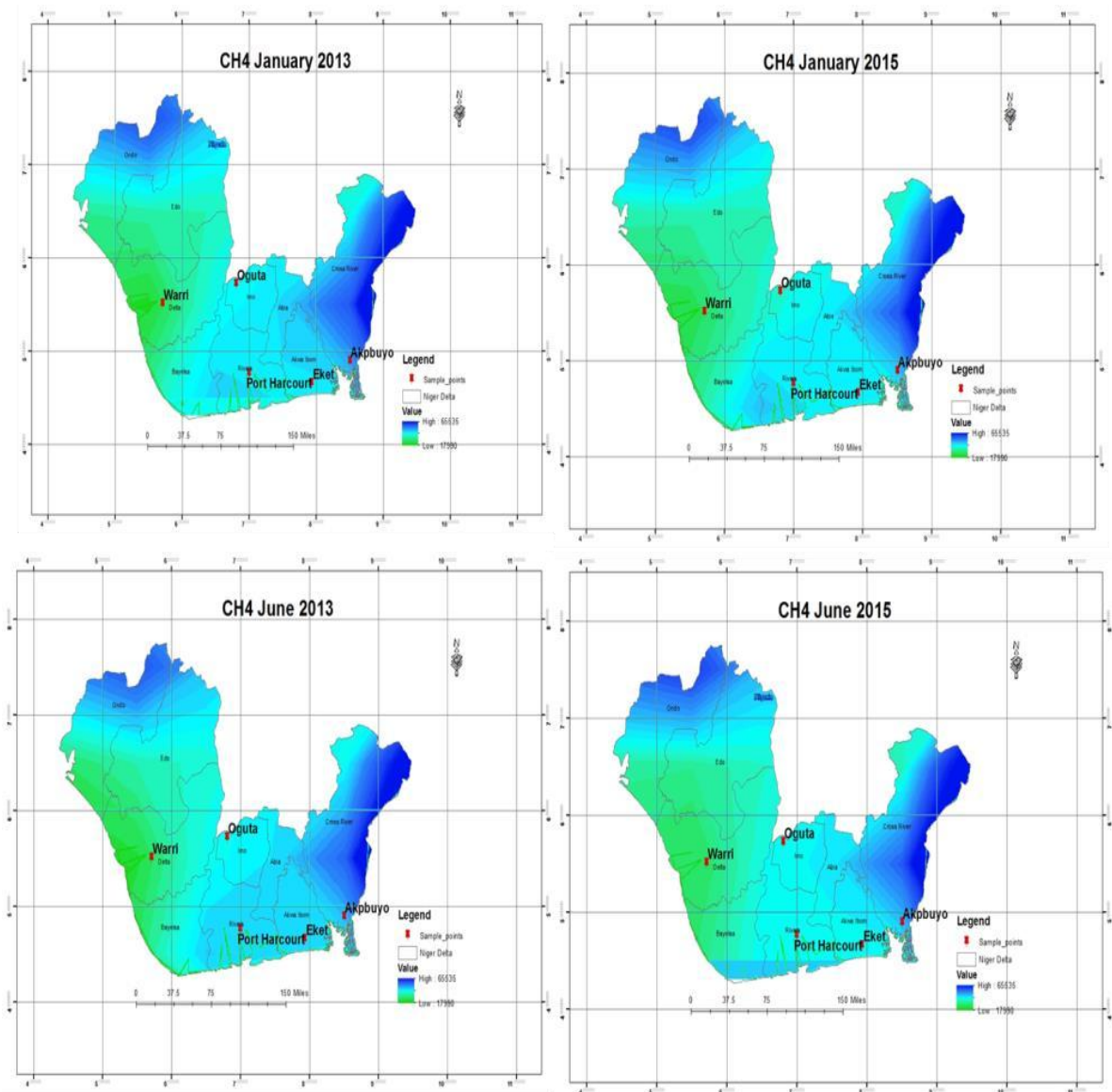
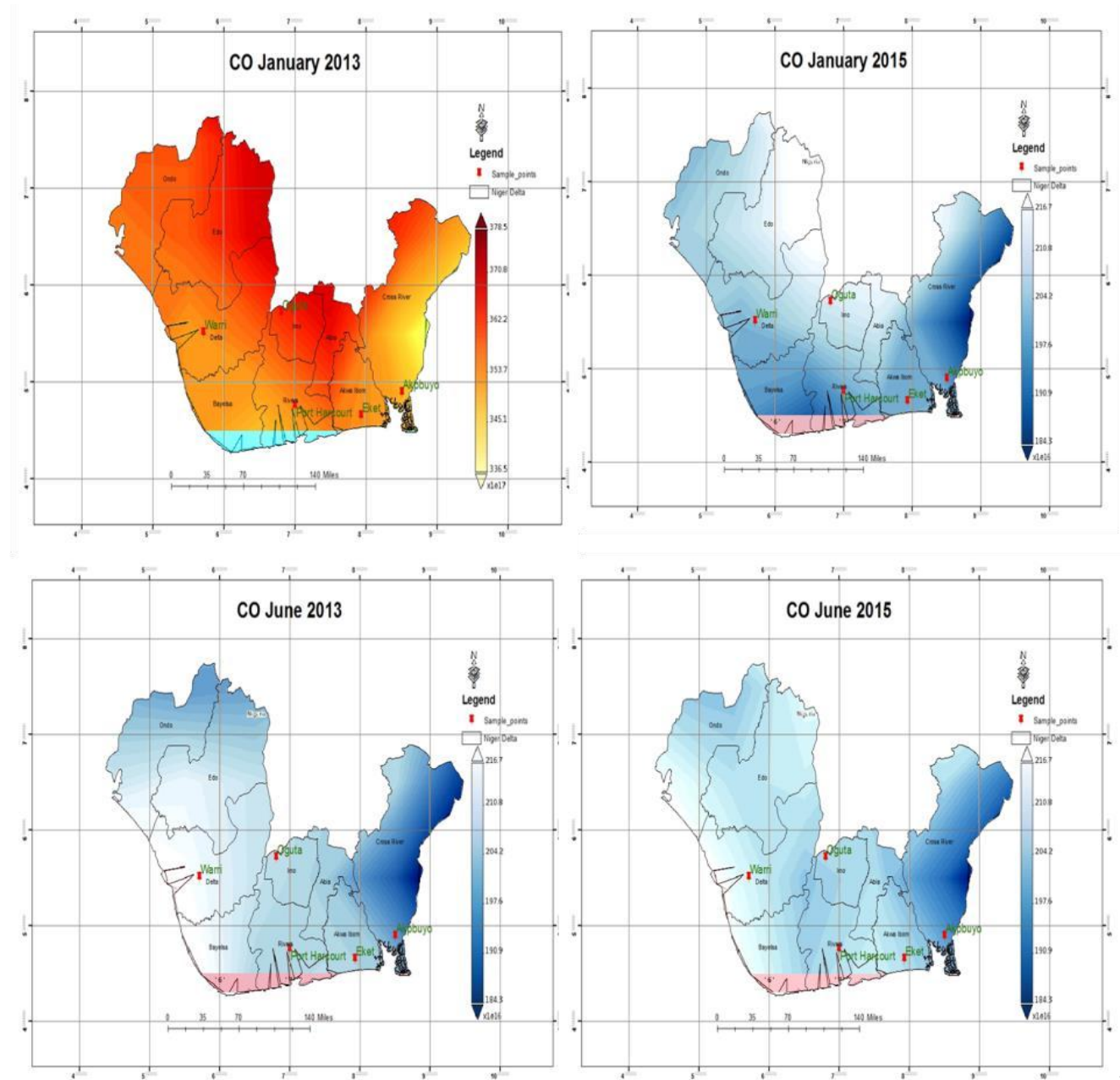


Figure 4.10: Spatial distribution of methane emission within the Niger Delta over the sample period

(ii) **Carbon Monoxide Emissions** : For CO, the order of variation is as follows; Oguta > Warri >Port Harcourt > Eket > Akpabuyo for Dry season 2013.



Figure

4.11: Spatial distribution of CO emission within the Niger Delta over the sample period.

**(iii) Nitrogen (iv) Oxide Emissions:**

The NO<sub>2</sub> emission concentrations in the dry season of Jan 2013 is very low, this is visible in the study locations with Oguta followed by Warri. The order of variation is; Oguta > Warri > Port Harcourt > Eket > Akpabuyo. In the wet season of Jun 2013, the concentration levels were less visible.

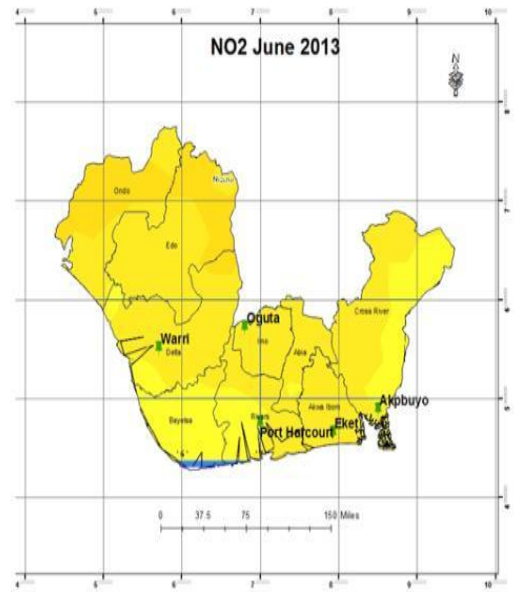
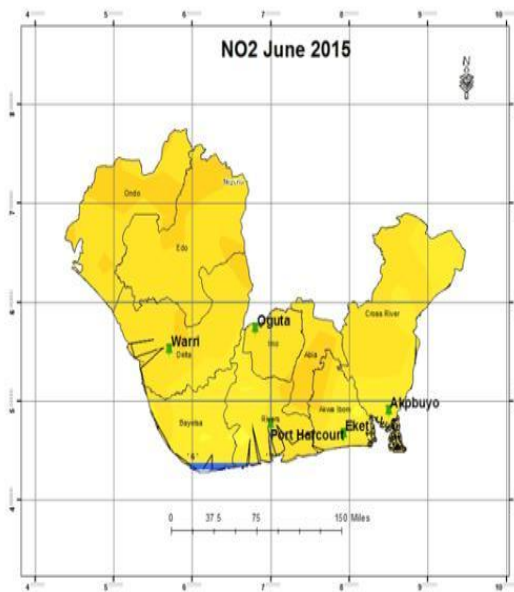
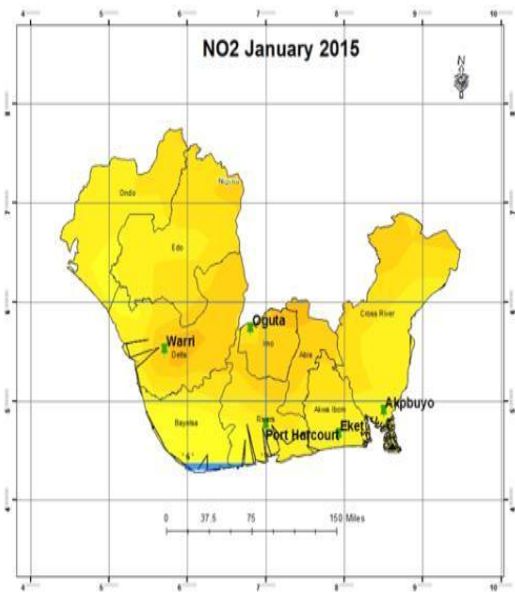
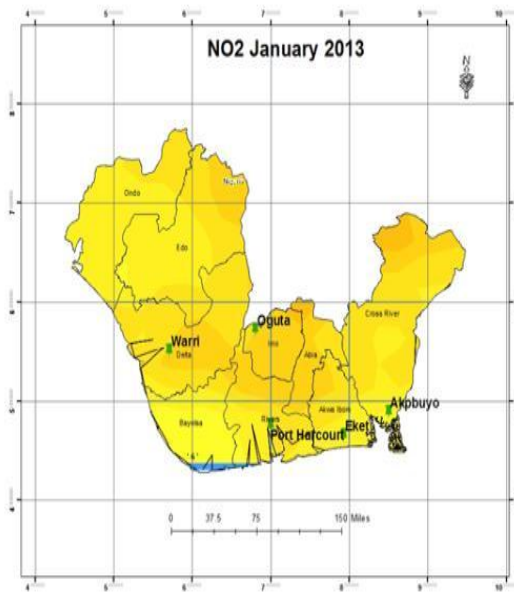


Figure 4.12: Spatial distribution of NO<sub>2</sub> emission within the Niger Delta over the sample period.

**(iv) Sulphur dioxide Emissions:** In the case of SO<sub>2</sub>, the dry season of 2013, the order of variation is as follows, Akpabuyo > Eket > Oguta > Port - Harcourt > Warri. In the wet season, the order of variation is Akpabuyo > Eket > Port- Harcourt > Warri > Oguta

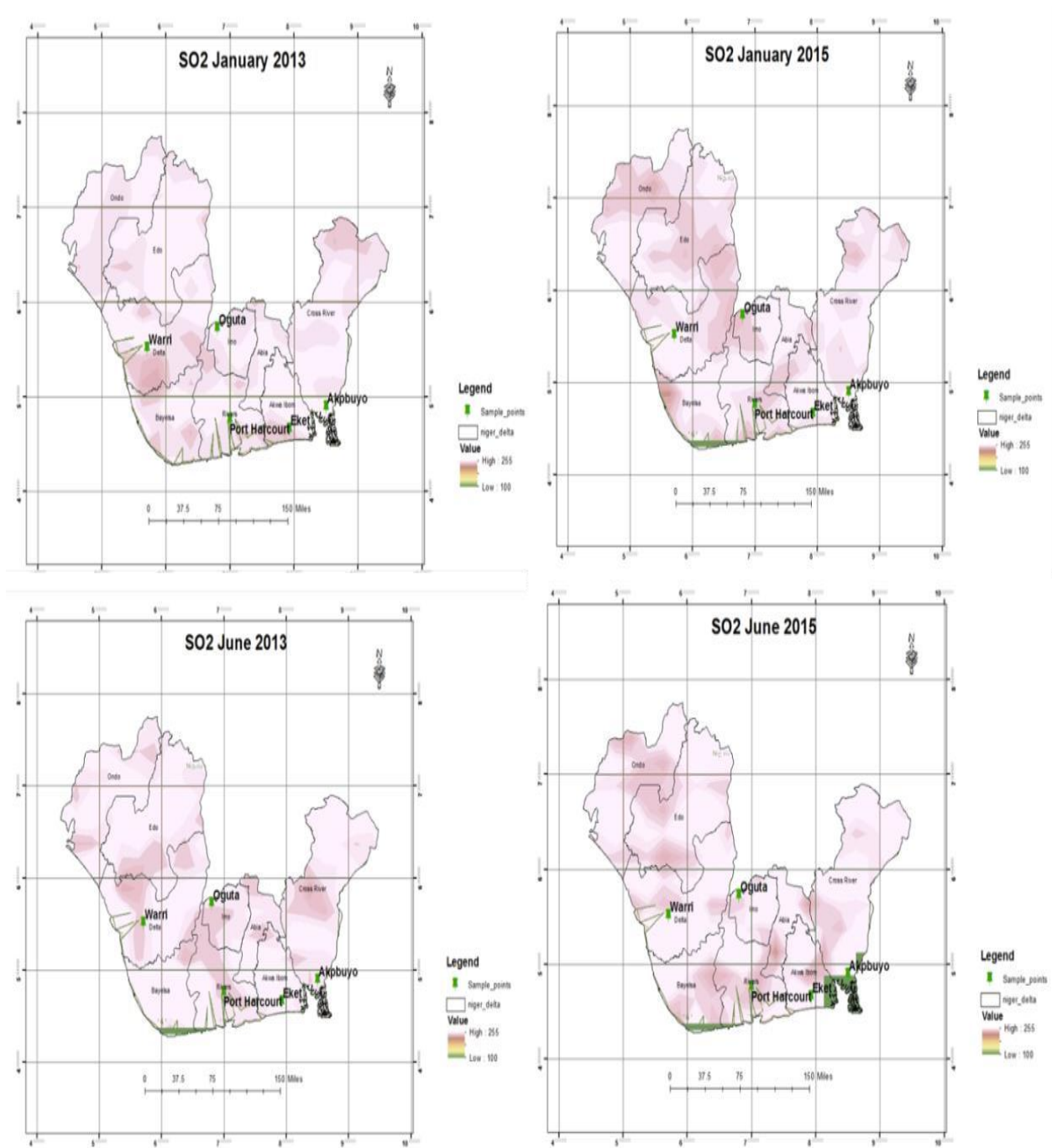


Figure 4.13: Spatial distribution of SO<sub>2</sub> emission within the Niger Delta over the sample period. The analysis of SO<sub>2</sub> concentrations across the study area indicates that the emission of this gas is very insignificant.

#### 4.1.3 Annual Variation of Species

**(A) Percentage (%) Difference:** The percentage (%) variation of the other atmospheric species are reported on table 4.2, the result implies that CH<sub>4</sub> and CO are the most abundant atmospheric gas among the four atmospheric gases studied. The further discussions on the variation of the individual species, which were not considered statistically different, were discussed below.

Table 4.2: Percentage (%) annual variation between 2013 and 2015

% Difference by year												
	CH <sub>4</sub>			NO <sub>2</sub>			SO <sub>2</sub>			CO		
Locat ion	2013	2015	% diff	2013	2015	% diff	2013	2015	% diff	2013	2015	% diff
<b>Port Harcourt</b>	1.23 E+2 1	9.8185 7E+20	<b>1.13</b> <b>E+0</b> <b>1</b>	- 3.93 E+3 1	- 4.31 E+3 1	- <b>4.62</b> <b>E+0</b> <b>0</b>	- 4.69 E+3 1	- 5.83 E+3 1	- <b>1.08</b> <b>E+0</b> <b>1</b>	8.79 E+1 9	9.07 E+1 9	- <b>1.54</b> <b>911</b>
<b>Eket</b>	1.08 E+2 1	1.0217 E+21	<b>2.94</b> <b>E+0</b> <b>0</b>	- 3.30 E+3 1	- 4.70 E+3 1	- <b>1.75</b> <b>E+0</b> <b>1</b>	- 4.83 E+3 1	- 6.10 E+3 1	- <b>1.16</b> <b>E+0</b> <b>1</b>	9.24 E+1 9	9.07 E+1 9	<b>0.93</b> <b>927</b> <b>5</b>
<b>Oguta</b>	1.24 E+2 1	1.06E +21	<b>7.83</b> <b>E+0</b> <b>0</b>	- 2.92 E+3 1	- 3.56 E+3 1	- <b>9.88</b> <b>E+0</b> <b>0</b>	- 4.19 E+3 1	- 4.83 E+3 1	- <b>7.10</b> <b>E+0</b> <b>0</b>	1.03 E+2 0	9.30 E+1 9	<b>5.10</b> <b>204</b> <b>1</b>
<b>Warri</b>	1.14 E+2 1	9.96E +20	<b>6.74</b> <b>E+0</b> <b>0</b>	- 3.68 E+3 1	- 3.81 E+3 1	- <b>1.74</b> <b>E+0</b> <b>0</b>	- 4.95 E+3 1	- 5.21 E+3 1	- <b>2.56</b> <b>E+0</b> <b>0</b>	1.03 E+2 0	8.87 E+1 9	<b>7.45 957</b> <b>2</b>
<b>Akpa buyo</b>	1.15 E+2 1	1.09E +21	<b>2.53</b> <b>E+0</b> <b>0</b>	- 2.79 E+3 1	- 3.17 E+3 1	- <b>6.38</b> <b>E+0</b> <b>0</b>	- 4.31 E+3 1	- 4.69 E+3 1	- <b>4.22</b> <b>E+0</b> <b>0</b>	1.12 E+2 0	1.05 E+2 0	<b>3.34</b> <b>296</b>

## (B) Mean Difference

Table 4.3: Statistical inference from the means of the years under study.

	<b>AK</b>	<b>Eket</b>	<b>Oguta</b>	<b>PHC</b>	<b>Warri</b>
	Zcal	Zcal	Zcal	Zcal	Zcal
<b>CH<sub>4</sub></b>	0.116	0.118	0.677	0.118	0.500
<b>CO</b>	0.432	0.134	0.653	0.983	0.885
<b>NO<sub>2</sub></b>	0.752	1.474	0.944	0.545	0.181
<b>SO<sub>2</sub></b>	0.742	1.803	0.931	1.769	0.574

The result shown in Table 4.3 was from the Z-test conducted for 2013 and 2015 emission concentrations at a 0.05 level significance and critical value of 1.96. The implication of the result is that over the years the variation in the emission concentrations is insignificant in all locations except for SO<sub>2</sub> which showed a significant variation in concentration in PHC and Eket, where the Z calculated were 1.76 and 1.8 respectively, Table 4.5 indicates that SO<sub>2</sub> increased from the 2013 value in PHC and Eket by 10.8% and 11.6% respectively. The percentage (%) variation of the other atmospheric species is reported in Table 4.5, the result implies that CH<sub>4</sub> and CO are the most abundant atmospheric gas among the four atmospheric gases studied.

### **(C) Comparison of Atmospheric Pollutants during Dry and Rain**

**Table 4.4 Variation between loadings during different seasons**

<div style="text-align: center;">% Difference Dry Vs Rain</div>												
<b>2013</b>												
<b>a</b>	CH <sub>4</sub>		% diff D vs R	NO <sub>2</sub>		% diff D vs R	SO <sub>2</sub>		% diff D vs R	CO		% diff D vs R
Port Harc ourt	5.99 E+20	6.32 E+20	- <b>2.69E</b> <b>+00</b>	- 1.27 E+31	- 2.66 E+31	- <b>3.55E</b> <b>+01</b>	- 1.65 E+31	- 3.04 E+31	- <b>2.97E</b> <b>+01</b>	6.02 E+19	1.94 E+18	<b>93.75</b>
Eket	5.63 E+20	5.21 E+20	<b>3.83E</b> <b>+00</b>	- 1.02 E+31	- 2.29 E+31	- <b>3.85E</b> <b>+01</b>	- 2.03 E+31	- 2.79 E+31	- <b>1.58E</b> <b>+01</b>	5.57 E+19	1.80 E+18	<b>93.75</b>
Ogut a	6.02 E+20	6.37 E+20	- <b>2.82E</b> <b>+00</b>	- 1.14 E+31	- 1.78 E+31	- <b>2.19E</b> <b>+01</b>	- 1.91 E+31	- 2.29 E+31	- <b>9.05E</b> <b>+00</b>	6.17 E+19	4.12 E+19	<b>19.9222</b> <b>5462</b>
Warr i	5.71 E+20	5.66 E+20	<b>4.40E-</b> <b>01</b>	- 1.27 E+31	- 2.41 E+31	- <b>3.10E</b> <b>+01</b>	- 1.78 E+31	- 3.18 E+31	- <b>2.82E</b> <b>+01</b>	6.09 E+19	4.17 E+19	<b>18.7134</b> <b>5029</b>
Akpa buyo	5.99 E+20	5.56 E+20	<b>3.72E</b> <b>+00</b>	- 1.27 E+31	- 1.52 E+31	- <b>8.96E</b> <b>+00</b>	- 2.03 E+31	- 2.30 E+31	- <b>6.24E</b> <b>+00</b>	6.79 E+19	4.45 E+19	<b>20.8185</b> <b>0534</b>
<b>2015</b>												
<b>b</b>	CH <sub>4</sub>			NO <sub>2</sub>			SO <sub>2</sub>			CO		
Port Harc ourt	5.69 E+20	4.13 E+20	<b>1.58E</b> <b>+01</b>	- 1.27 E+31	- 3.04 E+31	- <b>4.12E</b> <b>+01</b>	- 2.16 E+31	- 3.68 E+31	- <b>2.61E</b> <b>+01</b>	5.27 E+19	3.53 E+19	<b>19.7951</b> <b>5264</b>
Eket	5.33 E+20	4.89 E+20	<b>4.36E</b> <b>+00</b>	- 1.27 E+31	- 3.43 E+31	- <b>4.59E</b> <b>+01</b>	- 2.41 E+31	- 3.68 E+31	- <b>2.08E</b> <b>+01</b>	5.68 E+19	3.56 E+19	<b>22.9820</b> <b>3852</b>
Ogut a	5.35 E+20	5.27 E+20	<b>7.53E-</b> <b>01</b>	- 1.40 E+31	- 2.16 E+31	- <b>2.13E</b> <b>+01</b>	- 1.91 E+31	- 2.92 E+31	- <b>2.09E</b> <b>+01</b>	5.76 E+19	3.53 E+19	<b>24.0043</b> <b>0571</b>
Warr i	5.78 E+20	4.18 E+20	<b>1.61E</b> <b>+01</b>	- 1.40 E+31	- 2.41 E+31	- <b>2.65E</b> <b>+01</b>	- 2.16 E+31	- 3.05 E+31	- <b>1.71E</b> <b>+01</b>	5.67 E+19	3.20 E+19	<b>27.8466</b> <b>7418</b>
Akpa buyo	5.70 E+20	5.23 E+20	<b>4.32E</b> <b>+00</b>	- 1.52 E+31	- 1.65 E+31	- <b>4.10E</b> <b>+00</b>	- 6.13 E+29	- 2.79 E+31	- <b>9.57E</b> <b>+01</b>	6.51 E+19	3.96 E+19	<b>24.3035</b> <b>8068</b>

**(D) Comparison of Atmospheric Pollutants Between Dry and Rain**

**Table 4.5: Variation of loadings between Dry and Rain Seasons.**

Dry												
A	CH <sub>4</sub>			NO <sub>2</sub>			SO <sub>2</sub>			CO		
	2013	2015	% diff	2013	2015	% diff	2013	2015	% diff	2013	2015	% diff
Port Harcourt	5.99 E+20	5.69 E+20	<b>2.59483</b> <b>0617</b>	- 1.27E +31	- 1.27 E+31	<b>8.88178</b> <b>E-15</b>	- 1.65E +31	- 2.16E +31	- <b>13.3333</b> <b>3333</b>	6.02E +19	5.27E +19	<b>6.69003</b> <b>8915</b>
Eket	5.63 E+20	5.33 E+20	<b>2.69234</b> <b>2795</b>	- 1.02E +31	- 1.27 E+31	- <b>11.1111</b> <b>1111</b>	- 2.03E +31	- 2.41E +31	- <b>8.57142</b> <b>8571</b>	5.57E +19	5.68E +19	- <b>1.03111</b> <b>1111</b>
Oguta	6.02 E+20	5.35 E+20	<b>5.89270</b> <b>0088</b>	- 1.14E +31	- 1.40 E+31	- <b>10.2362</b> <b>2047</b>	- 1.91E +31	- 1.91E +31	<b>0</b>	6.17E +19	5.76E +19	<b>3.43671</b> <b>4166</b>
Warri	5.71 E+20	5.78 E+20	- <b>0.60922</b> <b>5413</b>	- 1.27E +31	- 1.40 E+31	- <b>4.86891</b> <b>3858</b>	- 1.78E +31	- 2.16E +31	- <b>9.64467</b> <b>0051</b>	6.09E +19	5.67E +19	<b>3.57142</b> <b>8571</b>
Akpabuyo	5.99 E+20	5.70 E+20	<b>2.46392</b> <b>3804</b>	- 1.27E +31	- 1.52 E+31	- <b>8.96057</b> <b>3477</b>	- 2.03E +31	- 6.13E +29	<b>94.1376</b> <b>1775</b>	6.79E +19	6.51E +19	<b>2.10042</b> <b>6822</b>
Rain												
B	CH <sub>4</sub>			NO <sub>2</sub>			SO <sub>2</sub>			CO		
	2013	2015	% diff	2013	2015	% diff	2013	2015	% diff	2013	2015	% diff
Port Harcourt	6.32 E+20	4.13E +20	<b>20.9</b>	- 2.66E+3 1	- 3.04E +31	<b>6.6</b> <b>7</b>	- 3.04E +31	- 3.68E+ 31	<b>-9.43</b>	4.08E +19	3.53E +19	<b>7.3</b>
Eket	5.21 E+20	4.89E +20	<b>3.22</b>	- 2.29E+3 1	- 3.43E +31	<b>-20</b>	- 2.79E +31	- 3.68E+ 31	<b>-13.7</b>	3.90E +19	3.56E +19	<b>4.5</b>
Oguta	6.37 E+20	5.27E +20	<b>9.45</b>	- 1.78E+3 1	- 2.16E +31	<b>-9.6</b>	- 2.29E +31	- 2.92E+ 31	<b>-12.1</b>	4.12E +19	3.53E +19	<b>7.7</b>
Warri	5.66 E+20	4.18E +20	<b>15</b>	- 2.41E+3 1	- 2.41E +31	<b>0.0</b>	- 3.18E +31	- 3.05E+ 31	<b>2.09</b>	4.17E +19	3.20E +19	<b>13.</b> <b>1</b>
Akpabuyo	5.56 E+20	5.23E +20	<b>3.06</b>	- 1.52E+3 1	- 1.65E +31	<b>-4.1</b>	- 2.30E +31	- 2.79E+ 31	<b>-9.63</b>	4.45E +19	3.96E +19	<b>5.7</b>

The yearly assessment study of the atmospheric gaseous concentrations in the selected regions revealed clear evidence in understanding the physical approaches of human contributions to climate variability, as well as the seasonal-gas relationship. Based on the observations of seasonal variations, PHC shows a significant of CH<sub>4</sub> in 2013. This corresponds to all the locations, signifying a high emission of methane in 2013. In 2015, there was a sharp reduction. A different result is seen in NO<sub>2</sub>, where 2015 shows a higher value than 2013 apart from Warri with zero recorded percentage difference. It can be deduced that at raining season, there is a linear relationship of the season with the gases.

**(D) Percentage (%) Difference in Locations**

**Table 4.6: Percentage Diff of Atmospheric Species in the Various Locations**

	CH <sub>4</sub>	Ref	Port			
Port Harcourt	5.99E+20	Harcourt	Eket	Oguta	Warri	
Eket	5.63E+20	3.13E+00				
Oguta	1.06E+21	-3.07E+01	-	3.07E+01		
Warri	9.96E+20	-2.49E+01	-	2.78E+01	3.11284	
Akpabuyo	1.09E+21	-2.92E+01	-	3.20E+01	-1.54052	4.65E+00
	NO <sub>2</sub>					
Port Harcourt		Ref Port Harcourt	Eket	Oguta	Warri	
Eket	-1.27E+31	11.01967858				
Oguta	-3.56E+31	-50.09503934	-55.5944			
Warri	-3.81E+31	-50.06939232	-37.9104	-3.39213		
Akpabuyo	-3.17E+31	-42.86837789	-30.8596	5.587393	9.169054	
	SO <sub>2</sub>					
Port Harcourt		Ref	Port			
Eket	-1.65E+31	Harcourt	Eket	Oguta	Warri	
Oguta	-2.03E+31	-10.43639414				
Warri	-4.83E+31	-49.12133495	-40.7753			
Akpabuyo	-5.21E+31	-51.94053065	-43.8829	-3.78486		
		-47.99746726	-39.5418	1.470588	5.252525	
	CO					
Port Harcourt		Ref	Port			
Eket	6.02E+19	Harcourt	Eket	Oguta	Warri	
Oguta	5.57E+19	3.927886031				
Warri	9.30E+19	-21.39240218	-25.1093			
Akpabuyo	8.87E+19	-19.12267426	-22.8787	2.366538		
		-26.99293249	-30.5964	-5.94375	-8.29861	

## 4.2 DISCUSSION

### (A) TIME SERIES

In figure 4.1, the time series plot for the various areas under investigation. The time series is plotted on the AIRS model for Methane and Carbon Monoxide. The result shows that December (dry season) is the peak of CH<sub>4</sub> emission in all the study locations with Warri having the highest value ( $3.86 \times 10^{19}$  mol/cm<sup>2</sup>), Port Harcourt ( $3.82 \times 10^{19}$  mol/cm<sup>2</sup>) Eket ( $3.80 \times 10^{19}$  mol/cm<sup>2</sup>), Oguta ( $3.79 \times 10^{19}$  mol/cm<sup>2</sup>), while the least value recorded in Akpabuyo ( $3.75 \times 10^{19}$  mol/cm<sup>2</sup>).

In figure 4.2, displays the time series plotted for SO<sub>2</sub> on the OMI mode. The curves showed that SO<sub>2</sub> is at its peak in the dry season between January and March each year with PHC having values between (0 - 0.5 mol/cm<sup>2</sup>), Warri (0.4 mol/cm<sup>2</sup>), Akpabuyo (0.4 mol/cm<sup>2</sup>), Oguta (0.3-0.5 mol/cm<sup>2</sup>), and Eket with the least value below -0.3 mol/cm<sup>2</sup>.

In figure 4.3, shows the CO emission time series on the AIRS model, the curves shows a distinct curve pattern in all the location, where emission increases from January-April, with Akpabuyo having the highest value ( $3.3 \times 10^{18}$  mol/cm<sup>2</sup>), Oguta ( $3.0 \times 10^{18}$  mol/cm<sup>2</sup>) Warri ( $2.95 \times 10^{18}$  mol/cm<sup>2</sup>), Eket ( $2.9 \times 10^{18}$  mol/cm<sup>2</sup>), PHC ( $2.8 \times 10^{18}$  mol/cm<sup>2</sup>). This analysis also shows that CO emission maintains double maxima in Nigeria at the peak of dry season and August-break.

The curves in figure 4.4 shows the NO<sub>2</sub> emissions in all the study locations plotted on the OMI Model maintain a January peak with the highest recorded in Oguta ( $5.3 \times 10^{15}$  l/cm<sup>2</sup>), PHC ( $5.2 \times 10^{15}$  l/cm<sup>2</sup>), Warri ( $4.9 \times 10^{15}$  l/cm<sup>2</sup>), Akpabuyo ( $4.7 \times 10^{15}$  l/cm<sup>2</sup>) and Eket with the least value of ( $4.6 \times 10^{15}$  l/cm<sup>2</sup>).

#### **4.2.1 HYSPLIT MODEL**

The result showed forward trajectory which gave the direction, concentration and where pollutants are deposited and specified location at an altitude of 0, 50, 100m above ground level (AGL).

The reduction in Port Harcourt and Oguta are related such that reduction in emission in Port Harcourt (PHC) results in a corresponding reduction in Oguta. The particles emitted in PHC are transported to Oguta as shown by the HYSPLIT model result in figures 4.5 and 4.6.

This model also shows that particles are likely dispersed towards North of Port Harcourt where Oguta is located due to wind speed regime and topography. Hence, Oguta receives enormous volume of gases from Port Harcourt. A look at the HYSPLIT model for Oguta showed that species have a maximum travel of distance of 10km.

The reference from the HYSPLIT model also revealed that gases from PHC and Warri are transported towards Oguta while emission from Eket is dispersed to Akpabuyo (see figure 4.7 and 4.8). This model also revealed that in Oguta and Akpabuyo, the gases are not dispersed beyond 10km from the source points while in the other locations they are dispersed up to a distance of 40km. (see Figure 4.9 and table 4.1).

#### **4.2.2 ANNUAL VARIATION OF SPECIES AND Z-TEST**

The difference between the mean of the individual gases for the two years was considered statistically significant when  $p < 0.05$  (see table 4.3). The total annual concentration of the individual gases is shown in table 4.1 with the accompanying difference between the two years. The result listed confirms the result arrived at in table 4.2, further discussion in the rate of change

over the years are as given above. The result listed in table 4.3, was arrived at from the Z-test conducted on the 2013 and 2015 emission concentrations at a 0.05 level of significance at a critical value of 1.96 using Microsoft Excel. The implication of the result is that over the years the variation in the emission concentrations is insignificant in all locations except for SO<sub>2</sub> which showed a significant variation in concentration in **PHC** and **Eket** where the Z calculated were 1.76 & 1.8 respectively, table 4.2 indicates that SO<sub>2</sub> increased from the 2013 value in **PHC** and **Eket** by 10.8% and 11.6%

#### **4.2.3 PERCENTAGE VARIATION OF SPECIES BETWEEN 2013 & 2015**

**(i) Methane (CH<sub>4</sub>):** The result from the analysis on table 4.2 shows that CH<sub>4</sub> is more abundant in 2013 than in 2015. This is given by the positive values recorded for the annual % difference calculated for the various locations. It was observed that Oguta recorded the highest CH<sub>4</sub> emission in 2013 at (1.24 x 10<sup>21</sup> mol/cm<sup>2</sup>), followed by Port Harcourt (1.23 x 10<sup>21</sup> mol/cm<sup>2</sup>) and Eket (1.08 x 10<sup>21</sup> mol/cm<sup>2</sup>). Meanwhile, in 2015 there was a reduction in CH<sub>4</sub> emission for all the locations. It was more obvious in Port Harcourt where 11.3% reduction was observed followed by Oguta 7.83%, Warri 6.74%, Eket 2.94% and Akpabuyo 2.53% (see figure 4.2). The reduced CH<sub>4</sub> emissions in all the studied locations may be attributed to a reduction in crude oil drilling and related activities in the Niger Delta area of Nigeria in 2015. This could be due to militant activities in 2015 Nigeria, that halted petroleum-related activities including gas flaring which is a major source of CH<sub>4</sub> emission in the study area (Obasi, 2016).

#### **(ii) Carbon Monoxide (CO)**

The CO trend shows that there is a slight increase in CO emission in Port Harcourt where the 2015 value was greater than 2013 by 1.549%. The result further showed that the 2013 loading

prevails over the 2015 loading in Akpabuyo by 3.34%, followed by Oguta (5.1%), Warri (7.45%) and Eket (0.93%) respectively.

### **(iii) Nitrogen (iv) Oxide (NO<sub>2</sub>)**

The NO<sub>2</sub> trend shows a general increase in emission rates in all the study locations with Eket having the highest volume in 2013 at (3.30 x10<sup>31</sup>mol/cm<sup>2</sup>) to 4.70x10<sup>31</sup>mol/cm<sup>2</sup>) in 2015 followed by Port Harcourt with a percentage difference of 4.62%,with Warri ,Oguta and Akpabuyo having percentage differences of 17.4%, 9.88%, 6.38% respectively.

### **(iv) Sulphur dioxide (SO<sub>2</sub>)**

There were major increases in emission rates from 2013 to 2015 with Oguta having a 7.1% increase, followed by Akpabuyo, Warri, Eket, Port Harcourt having values 4.2%,2.5% 1.1% and 1.08% respectively.

## **4.2.4 PERCENTAGE DIFFERENCE IN 2013 & 2015**

The result presented in tables 4.4 and 4.5 are the comparison of the seasonal values for the different years. In the first part (table 4.4), the variation in loading for the two seasons in the same year was considered, while in the second part (table 4.5), the loading for the same season but for the different years was also considered.

### **(i) Dry season against Rainy season**

**YEAR 2013:** The result of the comparison for 2013 shows that during the rainy season CH<sub>4</sub> was emitted more in Port Harcourt and Oguta at 2.69 % and 2.83% respectively. In the other

locations the dry season concentration was found to be greater than the rainy season values, in Eket 3.83%, Warri 4.4%, Akpabuyo 3.72% simultaneously.

The result also shows that CO loading decreased during the rainy season in all the locations. A breakdown of the differences show that the highest reduction occurred in Port Harcourt (93.7%) followed by Eket (93.7%), Akpabuyo (20.81%), Oguta (19.92%) and Warri (18.71%) (see table 4.4).

**YEAR 2015:** In 2015, the seasonal variation analysis shows that there was a significant reduction in the CH<sub>4</sub> emission. A breakdown of the result indicates that CH<sub>4</sub> reduced during the rainy season of 2015 in Port Harcourt by 15.8%, 4.36% in Eket, .75% in Oguta, 10.61% in Warri and Akpabuyo 4.32%.

Furthermore, there was a reduction in the CO emission during the rainy season of 2015 in all the study sites at varying percentages; 19.79% in PHC, 22.98% in Eket, 24% in Oguta, 27.84% in Warri and 24.3% in Akpabuyo (see table 4.4).

The results for the 2 years shows that the seasonal variation of CO was more prominent in Port Harcourt and Eket in 2013 than 2015 implying that more CO resided in the atmosphere during the rainy season of 2015 than 2013 in these two locations. For Oguta, Warri and Akpabuyo, there was reduced CO emission during the rainy season of 2015 compared with the 2013 value.

For both SO<sub>2</sub> and NO<sub>2</sub> the result in table 4.3 and 4.4 shows that during the rainy season of both years the concentration of both gases increased more than the dry season emission values (see table 4.5)

### **(ii) Dry season verses Dry season**

A comparison seasonal variation for the period under review same seasons but for the different years.

**Dry season:** Table 4.5 shows that the total volume of CH<sub>4</sub> emitted in 2013 outweighs the 2015 emission in all the study locations such that Port Harcourt recorded a 2.5% difference, Eket 2.6%, Oguta 5.8% and Akpabuyo 2.4%, subsequently the 2015 value was greater than 2013 value by 0.6% in Warri.

Furthermore, the result for NO<sub>2</sub> emission shows that in Eket, Oguta, Akpabuyo and Warri the NO<sub>2</sub> decreased at 11.11%, 10.23%, 8.96% and 4.86% respectively while an increase of was recorded in Port Harcourt at 8.88E-15%.

For SO<sub>2</sub>, the result showed an increased loading in Port Harcourt, Eket and Warri from the 2013 value by 13.33%, 8.57% and 9.64% respectively, while it reduced by 94.13% in Akpabuyo and remained neutral in Oguta.

Finally, the result for CO showed that a decrease in CO emission in Port Harcourt by 6.69%, Oguta 3.43%, Warri 3.57% and Akpabuyo 2.1%, while in Eket it increased by 1.03% (see table 4.5).

### **(iii) Rainy Season**

During the rainy season there was a reduction in CH<sub>4</sub> and CO concentration in all the study locations through wet deposition (see table 4.5). Furthermore, there was an increase in NO<sub>2</sub> and SO<sub>2</sub> loading over the study period in all locations except at Warri where the SO<sub>2</sub> loading decreased by 2.09% while NO<sub>2</sub> recorded a neutral value.

#### 4.2.5 Percentage (%) Difference in Locations

The variation of atmospheric species concentration in all locations where calculated and the result arrived at, is as presented on table 4.6. The analysis was carried out on the individual gases using the % difference formula by Onyeuwaoma (2015).

$$\% \text{ difference} = \left( \frac{T_{rl} - T_{ot}}{T_{rl} + T_{ot}} \right) \times 100 \quad . \quad 4.1$$

$T_{rl}$  : total in the reference location,       $T_{ot}$  : total in the other location.

#### Using Port Harcourt (PHC) as a reference location

The result shows that the volume of CH<sub>4</sub> in Oguta, Warri and Akpabuyo outweighs the value in PHC value by 30.7%, 24.9% and 29.2% respectively, while the volume occurrence in PHC outweighs that of Eket by 3.13%.

#### Using Eket as a reference location

With Eket, CH<sub>4</sub> value was compared with Oguta, Warri and Akpabuyo, the result shows that CH<sub>4</sub> occurred more at varying percentages, 30.7% in Oguta, 27.8% in Warri and 32% in Akpabuyo.

#### Using Oguta as a reference location

The magnitude of CH<sub>4</sub> concentration in Oguta compared against Warri and Akpabuyo indicates that there is 3.11% increase in CH<sub>4</sub> in Oguta over Warri, while the value increase in Akpabuyo was more by 1.54%.

**Using Warri as a reference location:** When the CH<sub>4</sub> value in Warri was compared with the value in Akpabuyo, the result shows that CH<sub>4</sub> occurred more in Akpabuyo compared to Warri by 4.65% (see Table 4.6).

**(ii) NO<sub>2</sub>**

Analysis of NO<sub>2</sub> variation over the various study sites showed that NO<sub>2</sub> is more abundant in Oguta (50%), Warri (50%) and Akpabuyo (42%) while in Eket the concentration is less by 11% when compared with Port Harcourt as a reference site.

When the value for Eket was compared with the value for Oguta, Warri and Akpabuyo, it was discovered that these locations had higher NO<sub>2</sub> emission within the period under study. Meanwhile, in Oguta it was observed that Warri had less NO<sub>2</sub> by 3.39%, while Akpabuyo had more NO<sub>2</sub> emission at 5.5%.

Subsequently, when the concentration for Akpabuyo emission was compared with Warri emission, it showed that the NO<sub>2</sub> in Akpabuyo recorded 9.16% emission higher than Warri.

Generally, the result shows that Warri had the highest NO<sub>2</sub> emission, followed by Oguta, Akpabuyo and Port Harcourt while Eket recorded the least value.

**(iii) SO<sub>2</sub>**

The analysis on SO<sub>2</sub> shows that the emission of this gas is very insignificant. Meanwhile, it was observed that Warri recorded the highest value followed by Oguta, Akpabuyo, Eket and lastly Port Harcourt (see table 4.6).

#### **(iv) CO**

The Percentage ( %) variation of CO emission in the study locations show that CO emission in Port Harcourt was greater than CO the emission in Eket by 3.92% and falls short in Warri, Oguta and Akpabuyo by 19.12%, 21.3% and 26.9% respectively.

In Eket, the CO emission was lower when compared with the values recorded in Oguta by 25.1%, 22.8% in Warri and 30.5% in Akpabuyo.

Subsequently, in Oguta it shows that Warri had more emission by 2.3% while Akpabuyo had more CO concentration by 5.94%. Furthermore, Akpabuyo had less emission over Warri by 8.2%. From these analyses the major atmospheric gases to contend with are CH<sub>4</sub> and CO while the occurrence of SO<sub>2</sub> and NO<sub>2</sub> are grossly insignificant (see table 4.5)

## CHAPTER FIVE

### CONCLUSION AND RECOMMENDATION

#### 5.1 CONCLUSION

An adequate study on a detailed characterization and dynamic modeling of tropospheric aerosols in parts of the Niger Delta was studied regarding SO<sub>2</sub>, CH<sub>4</sub>, CO, NO<sub>2</sub>. The study was conducted for a period of two (2) years within months of January 2013 and June 2015. The results revealed that CH<sub>4</sub> in Oguta, Warri, and Akpabuyo outweigh the value in Port Harcourt value by 30.7%, 24.9%, and 29.2% respectively, while the volume occurrence in Port Harcourt outweighs that of Eket by 3.13%. During the rainy season, there was a reduction in CH<sub>4</sub> and CO concentration in all the study locations due to wet depositions. Furthermore, there was an increase in NO<sub>2</sub> and SO<sub>2</sub> loading over the study period in all locations except at Warri where the SO<sub>2</sub> loading decreased by 2.09% while NO<sub>2</sub> recorded a neutral value. Temporal variations of the atmospheric pollutants were illuminated with time series models. This was accomplished to show the temporal correlation of the air pollutants with time, which could be useful for the prediction of atmospheric aerosols.

Spatial attributes of the atmospheric aerosols were determined which revealed areas with elevated values of the pollutants in a choropleth map layer. The result indicated elevated values of CH<sub>4</sub> observed in Akpabuyo followed by Port Harcourt. The order of variation is Akpabuyo > Port- Harcourt > Eket > Oguta > Warri for the Dry season of 2013. For the wet season, the concentration level remained the same except the order of variation changing, with Akpabuyo followed by both Eket and Port-Harcourt. The order of variation is as follows; Akpabuyo > Eket > Port Harcourt > Oguta > Warri in 2015, the order of variation is Akpabuyo > Port- Harcourt >

Eket > Oguta > Warri. But for the wet season, Port Harcourt, Eket and Oguta had almost the same concentration levels.

For CO, the order of variation is as follows; Oguta > Warri > Port Harcourt > Eket > Akpabuyo for dry season 2013. For the wet season of 2013, the order of variation is as follows; Warri > Oguta > Port- Harcourt > Eket > Akpabuyo. For the dry season of 2015, the order of variation changed with Warri having the highest value followed by Oguta. The order of variation is as follows; Warri > Oguta > Port- Harcourt > Eket > Akpabuyo. The wet season of 2015 shows the order of variation changed with Warri having the highest value followed by Oguta. The order of variation is as follows; Warri > Oguta > Port- Harcourt > Eket > Akpabuyo.

In the case of SO<sub>2</sub>, the dry season of 2013, the order of variation is as follows, Akpabuyo > Eket > Oguta > Port - Harcourt > Warri. In the wet season, the order of variation is Akpabuyo > Eket > Port- Harcourt > Warri > Oguta. For the dry season of 2015, the order of variation changed with Akpabuyo having the highest value followed by Eket. The order of variation is as follows; Akpabuyo > Eket > Port- Harcourt > Warri > Oguta. The wet season of 2015 shows the order of variation changed with Warri having the highest value followed by Oguta. The order of variation is as follows; Warri > Oguta > Port- Harcourt > Eket > Akpabuyo.

NO<sub>2</sub> emission concentrations in the dry season of Jan 2013 is very low, this is visible in the study locations with Oguta followed by Warri. The order of variation is; Oguta > Warri > Port Harcourt > Eket > Akpabuyo. In the wet season of Jun 2013, the concentration levels were less visible. The emission rates for 2015 are not pronounced, having low rates of emission. Both in the dry and wet seasons. The HYSPLIT model result showed forward trajectory which gave the direction, concentration and where pollutants are deposited and specified the location at an

altitude of 0, 50, 100m above ground level (AGL). The reduction in Port Harcourt and Oguta are related such that a reduction in emission in Port Harcourt (PHC) results in a corresponding reduction in Oguta. The particles emitted in PHC are transported to Oguta. This model shows that particles are dispensed towards the North of Port Harcourt where Oguta is located. Hence Oguta receives an enormous volume of gases from Port Harcourt. A look at the HYSPLIT model for Oguta showed that the species does not travel long distances before being deposited (deposited within 10km). This implies that pollutants deposited around Oguta and environs are from where most of them are generated. The reference from the HYSPLIT model also revealed that gases from PHC and Warri are transported towards Oguta while emission from Eket is dispersed to Akpabuyo. This model also revealed that in Oguta and Akpabuyo, the gases are not dispersed beyond 10km from the source points while in the other locations they are dispersed up to a distance of 40km. This could be attributed to the low elevation of Oguta and Akpabuyo since areas with low elevation seems to accumulate more air pollutants

## **5.2 RECOMMENDATION**

It is therefore, recommended that appropriate environmental legislation and measures for mitigation and reduction of atmospheric emission should be formulated in the study area for environmental sustainability.

## **CONTRIBUTIONS TO KNOWLEDGE**

It has been proven that seasonal variations have influence in the occurrence of these atmospheric aerosols in the various locations.

This work has also established the major sources of these aerosols such as gas flaring, crude oil mining.

## REFERENCES

- Acker, J., & Leptoukh, G, (2007). Online analysis enhances use of NASA Earth science data, *EOS. Transactions of American. Geophysical Union*, 88, 14-17.
- Adimula, I. A., Falaiye, O. A., & Adindu, C. L., (2008). Effects of aerosols loading in the atmosphere on the visibility changes in Ilorin, Nigeria. *Centre point* (Science Edition) 16, 15 -23.
- Andrews D.G, (2000). Introduction to Atmospheric Physics, Cambridge University Press, Cambridge.
- Anuforom, A.C., L.E. Akeh, P.N. Okeke, F.E. & Opara, O (2007). Inter-annual variability and long-term trend of UV-absorbing aerosols during the Harmattan season in sub-Saharan West Africa. *Atmospheric Environment*, 41, 1550–1559.
- Aumann, H. H., M.T. Chahine, C. Gautier, M.D. Goldberg, E. Kalnay, L.M. McMillin, H. Revercomb, P.W. Rosenkranz, W.L. Smith, D.H. Staelin, L.L. Strow, J. Susskind, (2003). AIRS/AMSU/HSB on the Aqua mission, Design, science objectives, data products, and processing systems, *IEEE Transactions on Geoscience and Remote Sensing*, 41, 253–264.
- Ayansina Ayanlade, Godwin Atai, Margaret Olusolape Jegede, (2019) Variability in atmospheric

aerosols and effects of humidity, wind and InterTropical discontinuity over different ecological zones in Nigeria, *Atmospheric Environment*, 201, 369-380, ISSN 1352-2310

Barnabas Morakinyo, Samantha Lavender, Victor Abbott. (2020) Retrieval of Land Surface Temperature from Earth Observation Satellites for Gas Flaring Sites in the Niger Delta, Nigeria. *International Journal of Environmental Monitoring and Analysis*. 8, 3, 59-74. doi: 10.11648/j.ijema.20200803.13

Batjes, N. H. (1996). Total carbon and nitrogen in the soils of the world. *European Journal of Soil Science*, 47, 151–163

Beer, C., Reichstein, M., Tomelleri, E., Ciais, P., Jung, M., Carvalhais, N., Rodenbeck, C., Arain, M., Baldocchi, D., Bonan, G., Bondeau, A., Cescatti, A., Lasslop, G., Lindroth, A., Lomas, M., Luysaert, S., Margolis, H., Oleson, K., Rouspard, O., & Papale, D. (2010). Terrestrial Gross Carbon Dioxide Uptake: Global Distribution and Covariation with Climate. *Science*. 329. 834-838. 10.1126/science.1184984.

Bhaga, Trisha D., Dube, Timothy; Shekede, Munyaradzi D Shoko & Cletah. (2020). "Impacts of Climate Variability and Drought on Surface Water Resources in Sub-Saharan Africa Using Remote Sensing. A Review" *Remote Sensing*. 12, 24: 4184. <https://doi.org/10.3390/rs12244184>.

Boucher, O., T. L. Anderson, (1995), GCM assessment of the sensitivity of direct climate forcing by anthropogenic sulfate aerosols to aerosol size and chemistry, *Journal of Geophysical Research*, 100,117–134.

Bouwman, L., Kees, K., Goldewijk, K.W. Van Der Hoek, A.H. W. Beusen, Detlef P. Van Vuuren, Jaap Willems, Mariana C. Rufino, & Elke, S. (2013) Exploring global changes in nitrogen and phosphorus cycles in agriculture induced by livestock production over the 1900–2050 period. *Proceedings of the National Academy of Sciences*, 110 (52) 20882–20887; DOI: 10.1073/pnas.1012878110.

Charlson, R.J., S.E. Schwartz, J.M. Hales, R.D. Cess, J.A. Coakley, J.E. Hansen, D.J. Hofmann, (1992): Climate forcing by anthropogenic aerosols. *Science*, 255, 423–430.

Chandrasekhar, S, 1960 . Radiative transfer . *A Dover Publications*. 1910-1995

Chiemeka, I.U., Oleka, M. O., & Chineke, T. C.(2007). Determination of Aerosol Metal Composition and Concentration During the 2004/2005 Harmattan Season at Uturu, Nigeria. *Advances in Science and Technology*, 1, 2 / 3, 126-132.

Conrad ,R. (1996) Soil microorganisms as controllers of atmospheric trace gases (H<sub>2</sub>, CO, CH<sub>4</sub>, OCS, N<sub>2</sub>O, and NO). *Microbiol Rev.*60(4):609-40. PMID: 8987358; PMCID: PMC239458.

Cotton,W.R (2000).Atmospheric Thermodynamics & Microphysics of Cloud Colorado:  
*Colorado State University.*

Daful, Mwanret Gideon, Adewuyi, Taiye Oluwafemia, Dadan-Garba, Aliyua, Oluwale,  
Olumide

Akinwumia, Muhammad, Muktar Namadib And Ezeamaka, Cyril Kanayochuku (2020)  
Apprising The Local and Global Implication of Ambient air Quality Index of Kaduna  
Metropolis, Nigeria *Original scientific article.* UDK: 502.3:613.15(669),  
614.71/.72(669) DOI: 10.5937/ZbDght2001022D

Draxler, Roland & Hess, G.. (1998). An overview of the HYSPLIT\_4 modeling system for  
trajectories, dispersion, and deposition. *Australian Meteorological Magazine.* 47. 295-  
308.<https://doi.org/10.1029/2008GL036394>

Husar R. B.(2006) Satellite Measurements of Atmospheric Aerosols,Washington University, St.  
Louis.

Haug, L. (2010). A Modeling Study of Seasonal and Inter-annual Variations of the Arctic Black  
Carbon and Sulphate Aerosols. *Ph.D. Thesis, Toronto,University of Toronto, Canada, 185.*

Intergovernmental Panel on Climate Change.(2007) C. A. Johnson. Cambridge; New York,  
Cambridge University Press: 289-348.

IPCC, (2013) Climate Change 2013: The Physical Science Basis. Contribution of Working Group

I to the Fifth Assessment Report of the Intergovernmental Panel on Climate Change [Stocker, T.F., D. Qin, G.-K. Plattner, M. Tignor, S.K. Allen, J. Boschung, A.

Nauels, Y. Xia, V. Bex and P.M. Midgley (eds.)]. Cambridge University Press, Cambridge, United Kingdom and New York, NY, USA, 1535 .

Jacob, J.D., (1999). Introduction to atmospheric chemistry. *Princeton University Press*.

Jacobson, R.L., (2003) *The Journal of Infectious Diseases*. 188

Li, L., Dubovik, O., Derimian, Y., Schuster, G. L., Lapyonok, T., Litvinov, P., Ducos, F., Fuertes,

D., Chen, C., Li, Z., Lopatin, A., Torres, B., & Che, H. (2019). Retrieval of aerosol components directly from satellite and ground-based measurements, *Atmospheric Chemistry. Physics*, 19, 13409–13443, <https://doi.org/10.5194/acp-19-13409-2019>,.

Lillesand, T. M., Kiefer, R. W., & Chipman, J. W. (2008). Remote Sensing and Image Interpretation, 6th ed. New York: Wiley.

Liu, Q., Hong, Y.-L. (2012). Comparison Of Aerosol Single Scattering Albedo Derived from the Ozone Monitoring Instrument with aerosol robotic network observations, *Atmospheric Oceanic Science Letters*, 5, 264–269.

Lu, D. G. Streets, B. de Foy, L. N. Lamsal, B. N. Duncan, & J. Xin, (2015). Emissions of nitrogen oxides from US urban areas: estimation from Ozone Monitoring Instrument retrievals for 2005–2014. *Atmospheric Chemistry and Physics*, Vol 15, 10367–10383.

McMurry, P.H., 2000. A review of atmospheric aerosol measurements. *Atmospheric Environment* 34,1959-1999

Morford, S., Houlton, B. & Dahlgren, R. Increased forest ecosystem carbon and nitrogen storage from nitrogen rich bedrock. *Nature* 477, 78–81. <https://doi.org/10.1038/nature10415>

Nwofor O. K. (2010). Rising Dust Aerosol Pollution at Ilorin in the Sub-sahel Inferred from 10-year Aeronet Data: Possible Links to Persisting Drought Conditions. *Research Journal of Environmental and Earth Sciences*, 2(4), 216-225,

Obiajunwa, E., Johnson-Fatokun, F., Olaniyi, B., & Olowole, A. (2002). Determination of the elemental composition of aerosol samples in the working environment of a secondary lead smelting company in Nigeria using EDXRF technique. *Nuclear Instruments & Methods in Physics Research Section B-beam Interactions With Materials and Atoms - NUCL INSTRUM METH PHYS RES B*. 194. 65-68. 10.1016/S0168-583X(02)00500-1.

Oluleye A, K.O. Ogunjobi, A. Bernard, V.O. Ajayi, A.A. Akinsanola, (2012). Multiyear Analysis of Ground-Based Sun photometer (AERONET) Aerosol Optical Properties and its Comparison with Satellite Observations over West Africa. *Global Journal of Human Social Science Geography & Environmental GeoSciences*,12, 31-48.

Oyediran K. Owoade , Olusegun G. Fawole , Felix S. Olise , Lasun T. Ogundele , Hezekiah B. Olaniyi , Marta S. Almeida , Manh-Dung Ho & Philip K. Hopke (2013) Characterization and source identification of airborne particulate loadings at receptor site-classes of Lagos Mega-City,Nigeria, *Journal of the Air & Waste Management Association*, 63:9, 1026-1035, DOI: 10.1080/10962247.2013.793627

Oyem, A.A., & Igbafe, A.I., (2010). Analysis of the Atmospheric Aerosol Loading over Nigeria. *Environmental Research Journal*,4, 145-156.

Pongratz, J., Raddatz , T., Reick, C. H., Esch, M., & Claussen, M.(2009) Radiative forcing from anthropogenic land cover change since A.D. 800. *Geophysical Research Letter*, 36, 2.

Prather, Michael, Holmes, Christopher & Hsu, Juno. (2012). Reactive greenhouse gas scenarios: Systematic exploration of uncertainties and the role of atmospheric chemistry. *Geophysical Research Letters*. 39. 9803-. 10.1029/2012GL051440.

Ramanathan V., P. J. Crutzen, J. T. Kiehl, D. Rosenfeld, (2001).Aerosols, Climate, and the Hydrological Cycle. *Science* 294, 2119 – 2124. DOI: 10.1126/science.1064034.

Reijers, T. J. A (2011). Stratigraphy and sedimentology of the Niger Delta. *Geologos*, 17(3): 133–162. doi: 10.2478/v10118-011-0008-3.

Short, K. C. & Stauble, A. J. (1967): Outline of geology of Niger Delta: *American Association of Petroleum Geologists Bulletin*, vol. 51, p. 761-779.

Suntharalingam, Parvatha, Buitenhuis, Erik, Le Quéré, Corinne, Dentener, Frank, Nevison, C., Butler, James , Bange, Hermann & Forster, Grant. (2012). Quantifying the Impact of Anthropogenic Nitrogen Deposition on Oceanic Nitrous Oxide. *Geophysical Research Letters*. 39. 10.1029/2011GL050778.

Tuttle, W. L. M., Brownfield, E. M. & Charpentier, R. R. (1999). The Niger Delta Petroleum System. Chapter A: Tertiary Niger Delta (Akata-Agbada) Petroleum System, Niger Delta Province, Nigeria, Cameroon and Equatorial Guinea, Africa. U.S. Geological Survey, Open File Report. 99-50-H.

Uchi, C. Nyigbem(2021) Assessment of Harmattan Dust Haze Over Northern Nigeria *Geography*  
Mhttp://bsuir.bsum.edu.ng:8080/jspui/handle/11409/806

Veefkind, V. A., & Lercher, J. A. (1999). on the elementary steps of acid zeolite catalyzed amination of light alcohols. *Applied catalysis A: general*, 181(2), 245-255.  
[https://doi.org/10.1016/S0926-860X\(98\)00408-6](https://doi.org/10.1016/S0926-860X(98)00408-6)

Woldai, Tsehaie. (2002). Geospatial Data Infrastructure: The Problem of Developing Metadata for

Geoinformation in Africa. In: *Proceedings of the 4th International conference of the African Association of Remote Sensing of the Environment AARSE: Geoinformation for sustainable development in Africa* : Abuja, Nigeria.

Yang, Y., Zhao, C., Wang, Q., Cong, Z., Yang, X., & Fan, H(2021).: Aerosol characteristics at the

three poles of the Earth as characterized by Cloud–Aerosol Lidar and Infrared Pathfinder Satellite Observations, *Atmospheric and Chemistry Physics.*, 21, 4849–4868, <https://doi.org/10.5194/acp-21-4849-2021>.